Published October 15, 2012



# Inhibition of tumor necrosis factor–related apoptosis-inducing ligand (TRAIL) reverses experimental pulmonary hypertension

Abdul G. Hameed,[1] Nadine D. Arnold,[1,3] Janet Chamberlain,[1] Josephine A. Pickworth,[1,3] Claudia Paiva,[1] Sarah Dawson,[1] Simon Cross,[2] Lu Long,[4] Lan Zhao,[5] Nicholas W. Morrell,[4] David C. Crossman,[1,3,6] Christopher M.H. Newman,[1] David G. Kiely,[3,7] Sheila E. Francis,[1] and Allan Lawrie[1]

[1]Department of Cardiovascular Science, [2]Department of Neuroscience, University of Sheffield, S10 2RX Sheffield, UK
[3]National Institute for Health Research Cardiovascular Biomedical Research Unit, S5 7AU Sheffield, UK
[4]Department of Medicine, University of Cambridge School of Clinical Medicine, Addenbrooke's and Papworth Hospital, CB2 0QQ Cambridge, UK
[5]Centre for Pharmacology and Therapeutics, Experimental Medicine, Imperial College London, W12 0NN London, UK
[6]Norwich Medical School, University of East Anglia, NR4 7TJ Norwich, UK
[7]Sheffield Pulmonary Vascular Disease Unit, Royal Hallamshire Hospital, S10 2JF Sheffield, UK

**Pulmonary arterial hypertension (PAH) is a life-threatening disease characterized by the progressive narrowing and occlusion of small pulmonary arteries. Current therapies fail to fully reverse this vascular remodeling. Identifying key pathways in disease pathogenesis is therefore required for the development of new-targeted therapeutics. We have previously reported tumor necrosis factor–related apoptosis-inducing ligand (TRAIL) immunoreactivity within pulmonary vascular lesions from patients with idiopathic PAH and animal models. Because TRAIL can induce both endothelial cell apoptosis and smooth muscle cell proliferation in the systemic circulation, we hypothesized that TRAIL is an important mediator in the pathogenesis of PAH. We demonstrate for the first time that TRAIL is a potent stimulus for pulmonary vascular remodeling in human cells and rodent models. Furthermore, antibody blockade or genetic deletion of TRAIL prevents the development of PAH in three independent rodent models. Finally, anti-TRAIL antibody treatment of rodents with established PAH reverses pulmonary vascular remodeling by reducing proliferation and inducing apoptosis, improves hemodynamic indices, and significantly increases survival. These preclinical investigations are the first to demonstrate the importance of TRAIL in PAH pathogenesis and highlight its potential as a novel therapeutic target to direct future translational therapies.**

CORRESPONDENCE
Allan Lawrie:
a.lawrie@sheffield.ac.uk

Abbreviations used: BMDC, BM-derived cell; BMT, BM transplantation; ePVRi, estimated pulmonary vascular resistance index; LVEDP, left ventricular end-diastolic pressure; LVESP, left ventricular end-systolic pressure; MCT, monocrotaline; PA AT, pulmonary artery acceleration time; PAH, pulmonary arterial hypertension; PAP, pulmonary artery pressure; PASMC, pulmonary artery SMC; PCNA, proliferating cell nuclear antigen; PH, pulmonary hypertension; PPARγ, peroxisome proliferator-activated receptor γ; RVEDP, right ventricular end-diastolic pressure; RVH, right ventricular hypertrophy; RVSP, right ventricular systolic pressure; SMA, smooth muscle actin; SMC, smooth muscle cell; TRAIL, TNF-related apoptosis-inducing ligand; TUNEL, TdT-mediated dUTP nick-end labeling.

Pulmonary arterial hypertension (PAH) is a devastating and life-threatening condition with high morbidity and mortality that often affects the young (Humbert, 2008). The disease is characterized by a progressive pulmonary vasculopathy that leads to an elevation in pulmonary artery pressure (PAP), right ventricular hypertrophy (RVH), and finally right ventricular failure (Chin et al., 2005; Hemnes and Champion, 2008; Humbert and McLaughlin, 2009). Pathologically, PAH is characterized by medial thickening, intimal fibrosis, and, in some cases, plexiform lesions of pulmonary arterioles. Multiple cell types are involved in this process, and evidence supports a central role for endothelial dysfunction followed by fibroblast and smooth muscle cell (SMC) proliferation and migration (Morrell et al., 2009). Current therapies are effective in relieving symptoms but provide only modest improvements in overall survival and do little to address the underlying cellular proliferation in PAH.

Our understanding of the molecular and cellular mechanisms involved in the pathogenesis of PAH has improved significantly over the



The Rockefeller University Press $30.00
J. Exp. Med. 2012 Vol. 209 No. 11 1919-1935
www.jem.org/cgi/doi/10.1084/jem.20112716

Supplemental Material can be found at:
http://jem.rupress.org/content/suppl/2012/10/11/jem.20112716.DC1.html

Published October 15, 2012



past decade, particularly because of the discovery of mutations in the BMPR2 (bone morphogenetic protein type 2 receptor; Lane et al., 2000). In addition, several growth factors such as PDGF (Schermuly et al., 2005; Perros et al., 2008), mitogens such as 5-Hydroxytriptamine and S100A4 (Lee et al., 1999; Lawrie et al., 2005), and cytokines such as IL-1 and IL-6 (Humbert et al., 1995; Steiner et al., 2009; Lawrie et al., 2011) have been implicated in the disease process, either in their own right or by interaction with the BMP signaling (Long et al., 2006; Hagen et al., 2007; Hansmann et al., 2008; Lawrie et al., 2008).

TNF-related apoptosis-inducing ligand (TRAIL; Apo2L) is a type II transmembrane protein whose transcripts are detected in a variety of human tissues, most predominantly in spleen, lung, and prostate (Wiley et al., 1995). They can be alternatively spliced to produce several different isoforms (Wang et al., 2011). There are four membrane TRAIL receptors, DR4 (death receptor 4, TRAIL-R1; Pan et al., 1997b), DR5 (TRAIL-R2; MacFarlane et al., 1997; Pan et al., 1997b; Screaton et al., 1997; Walczak et al., 1997), DcR1 (Decoy Receptor 1, TRAIL-R3; Degli-Esposti et al., 1997b; Pan et al., 1997a; LeBlanc and Ashkenazi, 2003), DcR2 (TRAIL-R4; Degli-Esposti et al., 1997a; Marsters et al., 1997; Pan et al., 1998), and the soluble protein OPG (osteoprotegerin) (Emery et al., 1998). In rodents, there is only one TRAIL death receptor (Wu et al., 1999). Both TRAIL-R1 and TRAIL-R2 contain a conserved DD (death domain) motif and mediate the extrinsic apoptosis pathway by TRAIL (Ashkenazi and Dixit, 1998). TRAIL-R3 lacks an intracellular domain and TRAIL-R4 has a truncated DD; both are therefore considered decoy receptors to antagonize TRAIL-induced apoptosis by competing for ligand binding along with OPG (Ashkenazi and Dixit, 1998; LeBlanc and Ashkenazi, 2003; Miyashita et al., 2004).

TRAIL has long been explored as an anti-cancer therapy (Wu, 2009) as a result of its innate ability to induce apoptosis in a variety of transformed or tumor cells while leaving normal, untransformed cells unaffected (Wiley et al., 1995; Pitti et al., 1996). Many cancer cells have subsequently been found to be resistant to TRAIL-induced apoptosis (Wu, 2009), the mechanism of which is not fully understood but may be dependent on the regulation and expression of TRAIL receptors by genetic (Pai et al., 1998) and epigenetic changes (Hopkins-Donaldson et al., 2003) as well as modulation of OPG expression (Holen and Shipman, 2006; De Toni et al., 2008).

TRAIL has also been shown to be important in the early resolution of inflammation (McGrath et al., 2011) and to have immunosuppressive and immunoregulatory functions that are important for lymphocyte homeostasis and the transition between innate-to-adaptive immunity (Falschlehner et al., 2009). Interactions between inflammation and vascular cells are a key aspect of vascular injury/repair and are considered to have an important role in cardiovascular disease. TRAIL mRNA and protein expression has previously been described in normal human pulmonary arteries (Gochuico et al., 2000). We have previously demonstrated that TRAIL protein is associated with concentric and plexiform pulmonary vascular lesions from patients with IPAH (Lawrie et al., 2008) and from a murine model of severe PAH (Lawrie et al., 2011). Other investigators have subsequently described pro-proliferative effects of TRAIL on systemic VSMC (Secchiero et al., 2004; Kavurma et al., 2008) and propose a role in neointimal formation in mice after a vascular injury (Chan et al., 2010) in atherosclerosis (Watt et al., 2011) and coagulation (Simoncini et al., 2009). However, its role in the pathogenesis of PAH had yet to be investigated. Interestingly, local inflammatory signals are also thought to play an important role in pulmonary vascular disease, and recent work has demonstrated that TRAIL can mediate the expression and release of proinflammatory cytokines from SMC (Song et al., 2011) as well as tumor cells (Tang et al., 2009) via activation of NF-κβ.

Because TRAIL protein expression is increased in pulmonary vascular lesions from both human and rodent models, we hypothesized that TRAIL is involved in the pathogenesis of PAH. To test this hypothesis, we sought to determine whether inhibition of TRAIL would have a beneficial effect on preclinical animal models and therefore represent a potential target for therapy in PAH.

We report here for the first time that expression of TRAIL is up-regulated in PA-SMCs isolated from patients with IPAH and that TRAIL is a mitogen and promigratory stimulus to human pulmonary artery SMCs (PASMCs) in vitro. We demonstrate that TRAIL is required for the development of PAH in three rodent models through blockade of TRAIL, either by genetic deletion (mouse) or with an anti-TRAIL antibody (rat). In addition, giving exogenous, recombinant TRAIL to the $ApoE^{-/-}/TRAIL^{-/-}$ mice resulted in the reestablishment of PAH. In intervention studies on models with established disease, TRAIL blockade significantly reduced pulmonary vascular remodeling and increased survival in a rat monocrotaline (MCT) model and in a murine model of severe PAH resulted in regression of pulmonary vascular remodeling with virtual normalization of right ventricular pressures. These therapeutic effects were associated with a reduction in proliferating cells and an increase in apoptotic cells within the distal pulmonary arteries and arterioles.

## RESULTS

### TRAIL expression is increased in PAH and induces proliferation and migration of PASMCs in vitro

TRAIL mRNA expression was significantly increased in PASMC explanted and grown in vitro from transplanted lungs of patients with IPAH compared with control patient cells (Fig. 1 A). The addition of rTRAIL to hPASMC in vitro resulted in a dose–response increase in both proliferation (Fig. 1 B) and migration (Fig. 1 C) with 30 ng/ml deemed to be the lowest dose with maximal effect. Because TRAIL naturally forms a homotrimer that binds to TRAIL receptors, we also examined the effect of using cross-linked TRAIL (anti-histidine antibody) and observed equivalent data (not depicted). We next examined the downstream signaling associated with rTRAIL-mediated

Published October 15, 2012



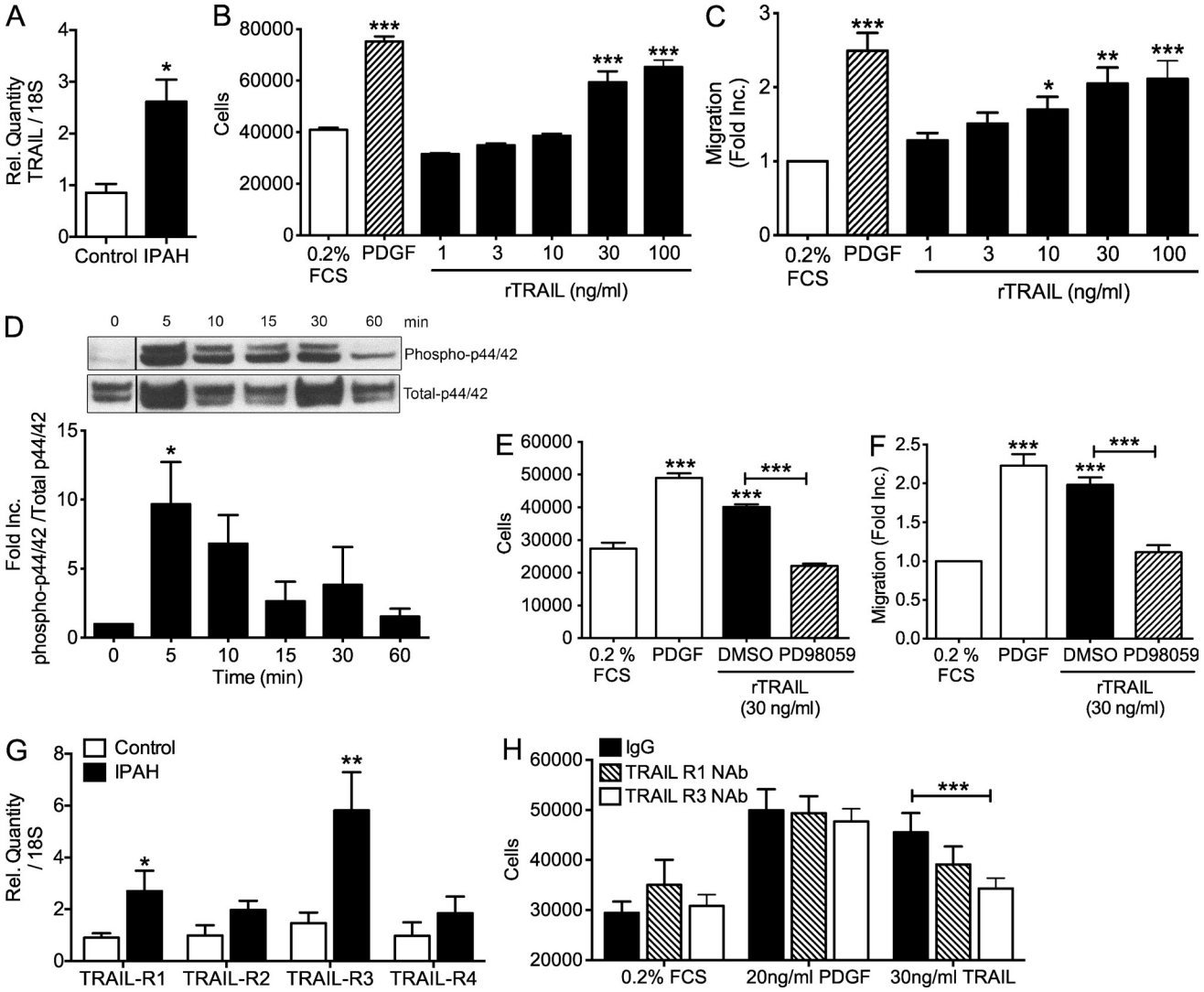


**Figure 1. TRAIL induces proliferation and migration of PASMCs.** (A) TaqMan expression of TRAIL in explanted PASMC from patients with IPAH normalized using ΔΔCT with 18S rRNA as the endogenous control gene. Human PA-SMCs were serum starved for 48 h before stimulation with 1–100 ng/ml of recombinant TRAIL or 10 ng/ml PDGF-BB. (B) Proliferation was assessed by cell counting at 72 h. (C) migration was measured at 6 h using a Boyden Chamber assay and normalized relative to unstimulated cells (0.2% FCS). (D) Time course of p42/44 / ERK1/2 phosphorylation in PASMC using 30 ng/ml of TRAIL. Black lines indicate that intervening lanes have been spliced out. (E and F) Treatment of PASMC with the ERK1/2 inhibitor PD98059 inhibited TRAIL (30 ng/ml)-induced proliferation (E) and migration (F). (G) TaqMan expression of TRAIL receptors in explanted PASMC from patients with IPAH normalized using ΔΔCT with 18S rRNA as the endogenous control gene. Human PA-SMCs were stimulated with 30 ng/ml of recombinant TRAIL or 20 ng/ml PDGF-BB with blocking antibodies for TRAIL-R1, TRAIL-R3, or an IgG control. (H) Proliferation of human PA-SMCs in response to 30 ng/ml of recombinant TRAIL or 20 ng/ml PDGF-BB after preincubation with IgG or neutralizing antibodies for TRAIL-R1, TRAIL-R3, or an IgG control. Error bars represent mean ± SEM, and all experiments were performed in triplicate. For data using patient material (A and G), $n = 3$. All remaining figures, $n = 5$. *, $P < 0.05$; **, $P < 0.01$; ***, $P < 0.001$, compared with 0.2% FCS, control, or 0 h samples.

proliferation and migration. Addition of 30 ng/ml TRAIL resulted in a significant increase in the phosphorylation of the extracellular regulated kinase 1/2 (Fig. 1 D), and the addition of the specific inhibitor PD98059 resulted in an inhibition of both TRAIL-mediated proliferation (Fig. 1 E) and migration (Fig. 1 F). Previous studies have implicated both TRAIL-R1 and TRAIL-R3 in the proliferative response to TRAIL in systemic SMC (Kavurma et al., 2008). We examined the expression of all known cell surface TRAIL receptors and found that TRAIL-R1 and, predominantly, TRAIL-R3 was significantly elevated in patient cells (Fig. 1 G). Furthermore, we demonstrate significantly attenuated TRAIL-induced proliferation of PASMC with antibody neutralization of TRAIL-R3 (Fig. 1 H).

### TRAIL expression in pulmonary arterioles increases with development of PAH in the MCT rat model

We have previously described the presence of TRAIL protein expression within pulmonary vascular lesions of both end-stage transplanted human and experimental model mouse lungs. To determine both the spatial and temporal expression of TRAIL in PAH pathogenesis, we initiated a time course of disease using the

Published October 15, 2012



MCT rat model of disease. Histological and immunohistochemistry analysis of serial lung tissue samples revealed evidence of pulmonary vascular remodeling from day 14, leading to progressive muscularization in the small resistance pulmonary arteries and arterioles (<50 µm) in MCT-treated rats (Fig. 2). TRAIL immunoreactivity was observed in epithelial and endothelial cells of saline-treated animals at all time points. There was an increase in the medial and perivascular tissue from around day 21 in the MCT-treated rats that coincided with the peak of pulmonary vascular remodeling and hemodynamic alterations associated with this model.

### Treatment with an anti-TRAIL antibody prevents the development of PAH in the MCT rat model

Because TRAIL expression increased with disease progression, we next aimed to determine whether blocking endogenous TRAIL with an anti-TRAIL antibody would modulate the development of PAH in the MCT rat model. Rats were injected with MCT and randomly assigned into two groups, one receiving an anti-TRAIL antibody and the other receiving an IgG isotype control, for 14 d via a subcutaneous osmotic mini-pump. Rats treated with IgG developed PAH, as defined by elevated right ventricular systolic pressure (RVSP), right ventricular end-diastolic pressure (RVEDP), reduced pulmonary artery acceleration time (PA AT), increased estimated pulmonary vascular resistance index (ePVRi), and decreased cardiac index (compared with saline treated rats; Table S2), whereas rats that received the anti-TRAIL antibody treatment had a normal RVSP (Fig. 3 A), RVEDP (Fig. 3 B), PA AT (Fig. 3 E), increased cardiac index (Fig. 3 F), reduced ePVRi (Fig. 3 G), and RVH (Fig. 3 H) 21 d after MCT injection. There was no significant difference in left ventricular hemodynamics (Fig. 3, C and D). The anti-TRAIL antibody–treated rats also showed significant reduction in the degree of pulmonary vascular remodeling as measured by media/cross-sectional area (Fig. 3, I and L), which was associated with a significant reduction in proliferation (Fig. 3, J and L) and an increase in apoptosis in the small pulmonary arteries and arterioles (Fig. 3, K and L). No increase in apoptosis of systemic vasculature tissue was observed (unpublished data).

### TRAIL$^{-/-}$ mice are protected from chronic hypoxia-induced pulmonary hypertension (PH)

To test whether the loss of TRAIL expression would prevent the development of PH in a murine model, we exposed male TRAIL$^{-/-}$ mice to 2 wk of chronic hypoxia (10% $O_2$). C57BL/6 control mice developed significant increases in RVSP (38.9 ± 2.6 mm Hg; Fig. 4 A), mildly raised RVEDP (Fig. 4 B), significantly reduced PA AT (Fig. 4 E) and cardiac index (Fig. 4 F), and significantly increased ePVRi (Fig. 5 G) compared with normoxic controls (Table S3). Pulmonary vascular remodeling of the small arterioles comprising smooth muscle actin (SMA)–positive cells was also observed in hypoxia-stimulated C57BL/6 mice (Fig. 4, I–K). In stark contrast, there was no evidence of PH in either the normoxic or hypoxic TRAIL$^{-/-}$ mice (Fig. 4, A–K). There was no evidence of any alterations in left ventricular hemodynamics between either genotype or hypoxia exposure (Fig. 4, C and D).

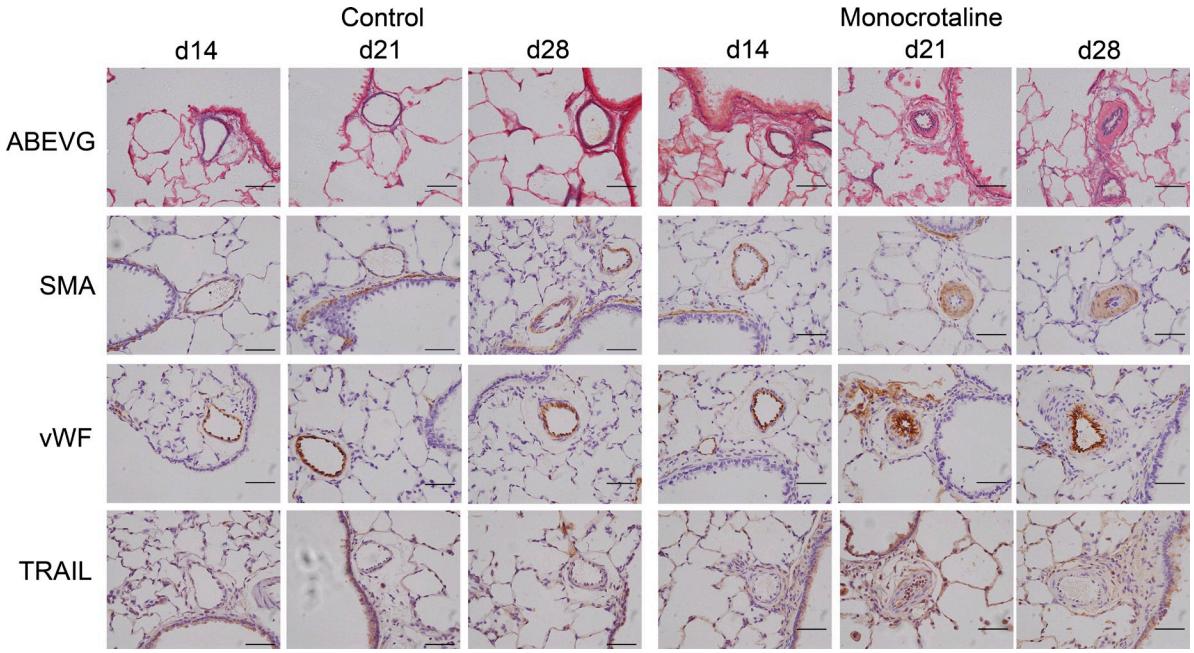


**Figure 2. TRAIL expression in pulmonary arterioles increases with pulmonary vascular remodeling in the MCT rat model.** Representative photomicrographs of serial lung sections from saline- and MCT-treated rats 14, 21, and 28 d after injection. Sections were stained with Alcian Blue Elastic van Gieson (ABEVG) or immunostained for α-SMA, von Willebrand factor (vWF), or TRAIL. TRAIL-expressing cells are present within the media and perivascular regions of remodeled small pulmonary arteries. All images are representative of $n = 7$ rats per group at each time point. Bars, 50 µm.

Published October 15, 2012



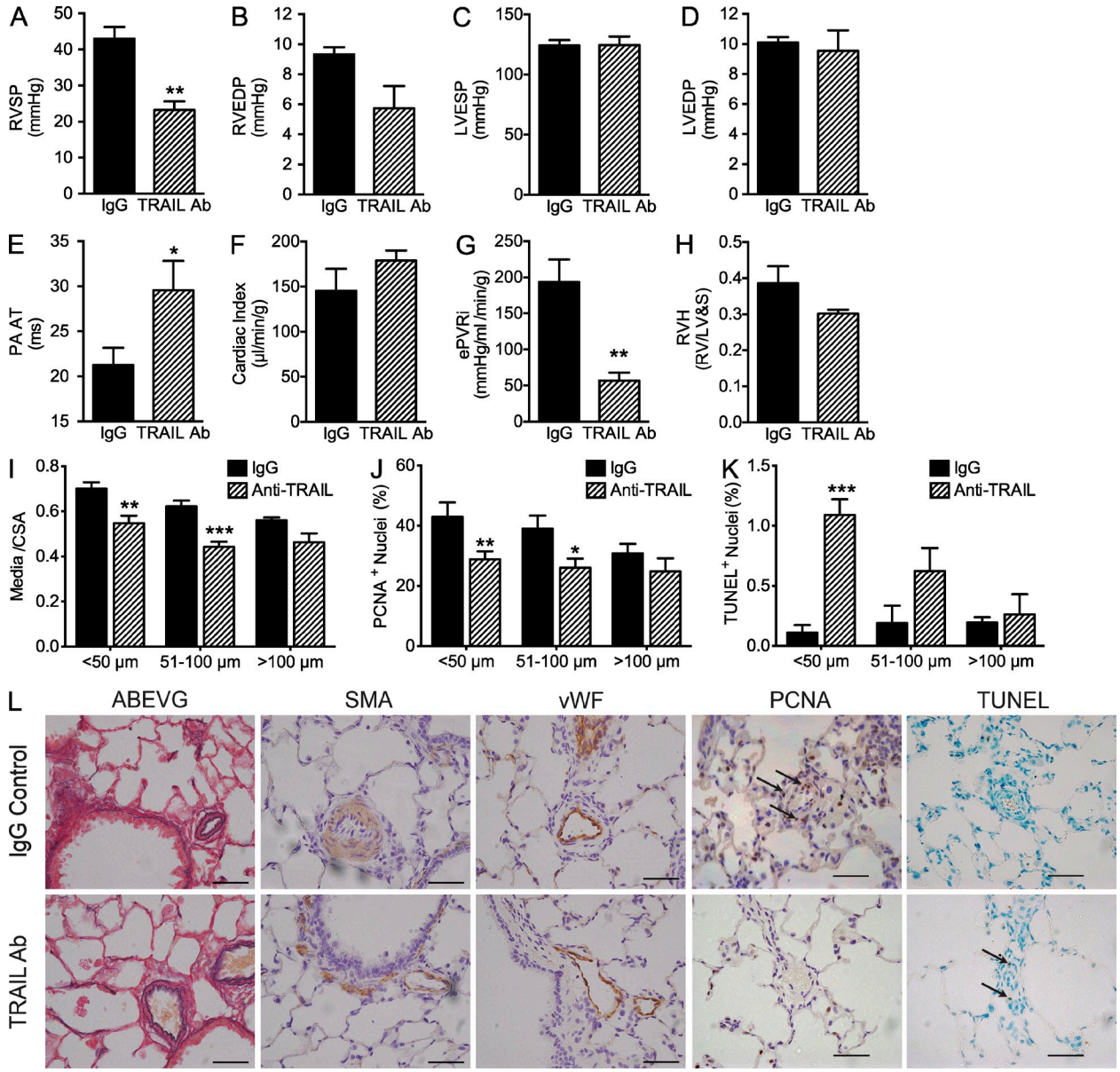


**Figure 3. Anti-TRAIL antibody treatment prevents the development of PAH at day 21 in the MCT rat model.** (A–D) Bar graphs show RVSP (A), RVEDP (B), left ventricular end-systolic pressure (LVESP; C), and LVEDP (D), measured in mm Hg. (E–H) PA AT (E), cardiac index (F), ePVRi (G), and RVH (H) are shown. (I) The degree of medial wall thickness as a ratio of total vessel size (Media/CSA). (J and K) Quantification of the percentage of proliferating cells (PCNA positive; J) and apoptotic (TUNEL positive; K) separated into pulmonary arteries <50 µm in diameter, vessels from 51 to 100 µm in diameter, and vessels >100 µm in diameter. (L) Representative photomicrographs of serial lung sections from IgG and anti-TRAIL–treated MCT-induced rats 21 d after injection. Sections were stained with Alcian Blue Elastic van Gieson (ABEVG) or immunostained for α-SMA, von Willebrand factor (vWF), PCNA, or TUNEL. Error bars represent mean ± SEM, $n = 4$ animals per group. *, $P < 0.05$; **, $P < 0.01$; ***, $P < 0.001$, compared with IgG-treated rats. Arrows point to PCNA- or TUNEL-positive cells. Bars, 50 µm.

### TRAIL is required and is sufficient for the development of PAH in the Paigen diet–fed ApoE$^{-/-}$ mouse model

We have previously reported that ApoE$^{-/-}$ mice fed the Paigen diet for 8 wk developed severe PAH consisting of substantial increases in RVSP associated with obliterative neointimal pulmonary vascular lesions that share many features with the human disease. As this model produced a severe pulmonary vasculopathy that was associated with TRAIL immunoreactivity (Lawrie et al., 2011), we next sought to determine whether TRAIL also had a critical role in this model. Using mice that were double deficient for ApoE and TRAIL (ApoE$^{-/-}$/TRAIL$^{-/-}$; Watt et al., 2011), we examined if TRAIL was similarly required for development of PAH.

Consistent with previous data (Lawrie et al., 2011), significant increases in RVSP (50.2 ± 3.5 mm Hg; Fig. 5 A) and RVEDP (Fig. 5 B), reduced PA AT (Fig. 5 E) and cardiac index (Fig. 5 F),

Published October 15, 2012



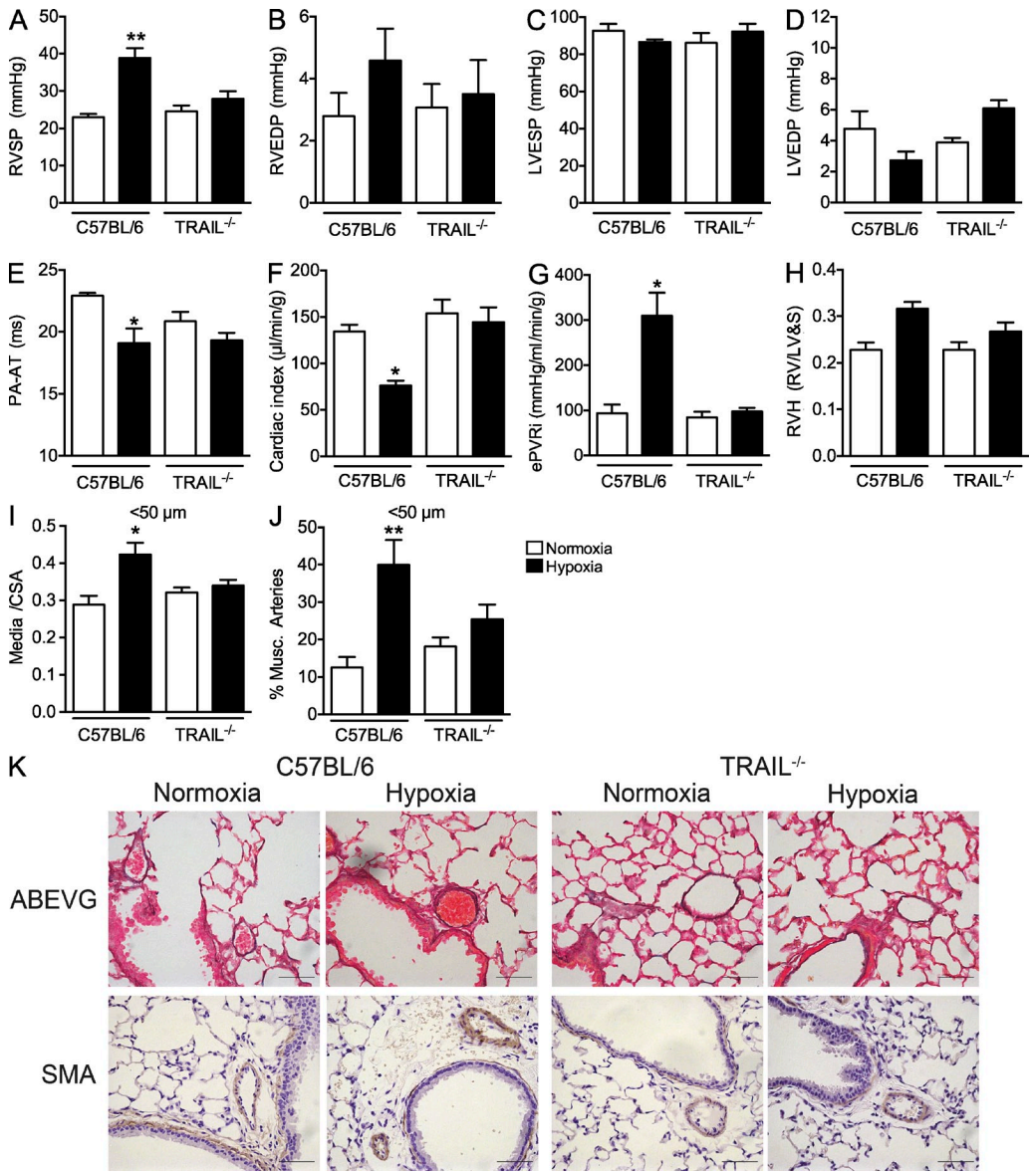


**Figure 4. TRAIL$^{-/-}$ mice are protected from chronic hypoxia–induced PH.** (A–D) Bar graphs show (A) RVSP, (B) RVEDP, (C) LVESP, and (D) LVEDP, measured in mm Hg. (E–H) PA AT (E), cardiac index (F), ePVRi (G), and RVH (H) are shown. (I) The degree of medial wall thickness as a ratio of total vessel size (Media/CSA). (J) The percentage of thickened pulmonary arteries <50 µm in diameter. (K) Representative photomicrographs of serial lung sections from C57BL/6 and TRAIL$^{-/-}$ mice after 2 wk of exposure to either room air or hypoxia. Sections were stained with Alcian Blue Elastic van Gieson (ABEVG) or immunostained for α-SMA. Error bars represent mean ± SEM, $n$ = 6–7 animals per group. *, $P < 0.05$; **, $P < 0.01$, compared with normoxic mice. Bars, 50 µm.

and increased ePVRi (Fig. 5 G) were observed in ApoE$^{-/-}$ mice after 8 wk on the Paigen diet. Also as previously reported (Lawrie et al., 2011), there was no significant difference in left ventricular hemodynamics (Fig. 4, C and D). There was no evidence of PH in either the chow- or Paigen diet–fed TRAIL$^{-/-}$ mice. Remarkably, ApoE$^{-/-}$ mice that were also deficient for TRAIL (ApoE$^{-/-}$/TRAIL$^{-/-}$) and fed the Paigen diet were protected from developing a significant increase in RVSP (27.8 ± 3.2 mm Hg; Fig. 5 A) or other changes in other hemodynamic markers of PAH (Fig. 5, A–G; Table S4). As with our previous data, despite the substantial pulmonary vascular remodeling and moderate increase in RVSP there was no significant effect of diet on RVH (Fig. 5 H). Severe pulmonary vascular remodeling of the small arteries and arterioles comprising SMA-positive cells was observed in the Paigen diet-fed ApoE$^{-/-}$ mice compared with their chow-fed littermates (Fig. 5, I and J). In contrast, neither the TRAIL$^{-/-}$ nor the ApoE$^{-/-}$/TRAIL$^{-/-}$ mice fed either chow or Paigen diet demonstrated any evidence of pulmonary vascular remodeling (Fig. 5, I and J).

We next investigated whether adding back recombinant TRAIL to the ApoE$^{-/-}$/TRAIL$^{-/-}$ mice would result in any alteration of the protected phenotype. ApoE$^{-/-}$/TRAIL$^{-/-}$

Published October 15, 2012



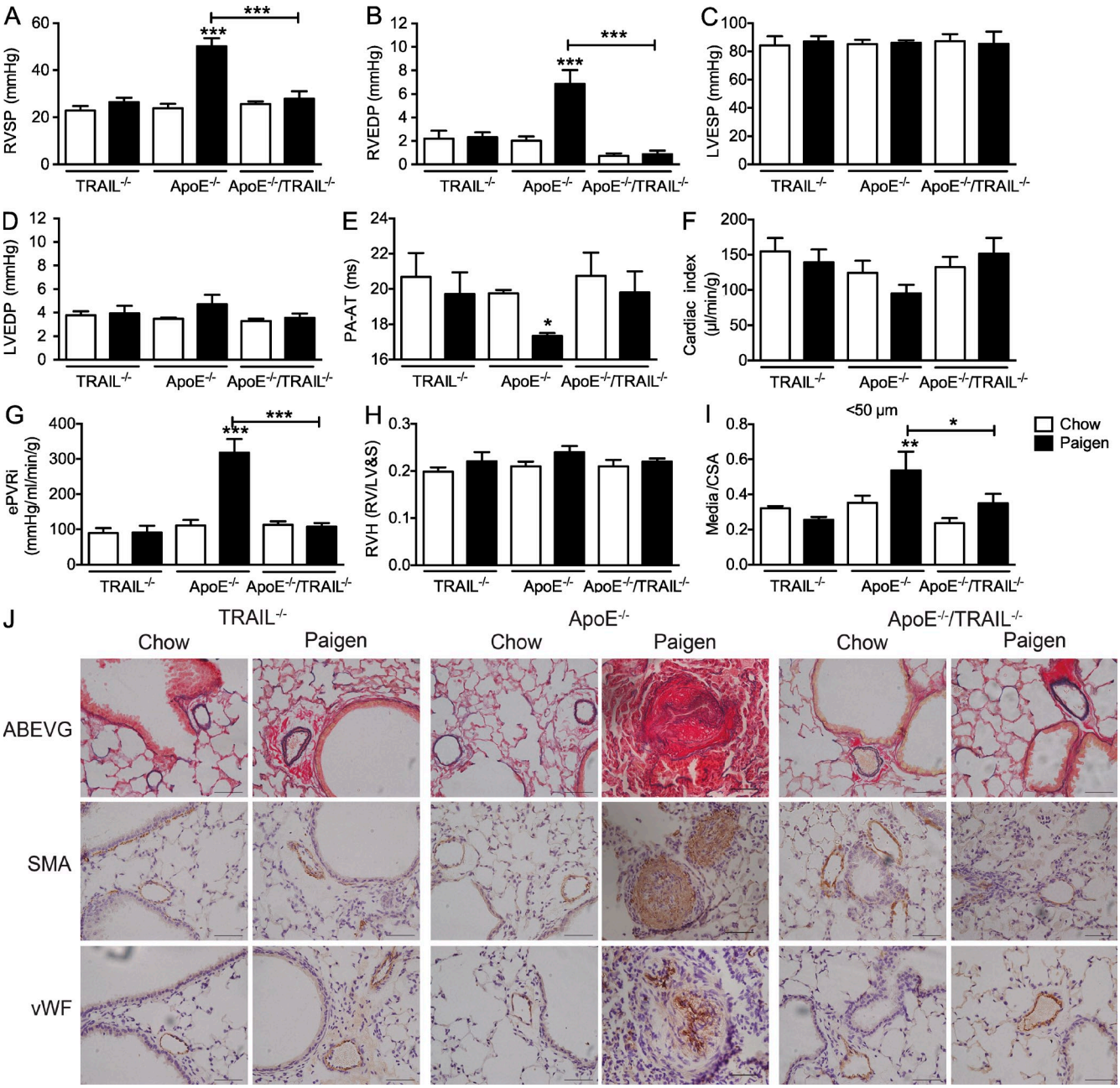


**Figure 5. ApoE$^{-/-}$/TRAIL$^{-/-}$ mice are protected from the development of PAH.** (A–D) Bar graphs show RVSP (A), RVEDP (B), LVESP (C), and LVEDP (D), measured in mm Hg. (E–H) PA AT (E), cardiac index (F), ePVRi (G), and RVH (H) are shown. (I) The degree of medial wall thickness as a ratio of total vessel size (Media/CSA) in pulmonary arteries <50 µm in diameter. (J) Representative photomicrographs of serial lung sections from TRAIL$^{-/-}$, ApoE$^{-/-}$, and ApoE$^{-/-}$/TRAIL$^{-/-}$ mice fed on either regular chow or Paigen diet for 8 wk. Sections were stained with Alcian Blue Elastic van Gieson (ABEVG) or immunostained for α-SMA or von Willebrand factor (vWF). Error bars represent mean ± SEM, *n* = 4–7 animals per group. *, P < 0.05; **, P < 0.01; ***, P < 0.001, compared with chow-fed mice. Bars, 50 µm.

mice were randomized into two groups and implanted with osmotic micro-pumps to deliver either recombinant mouse TRAIL or saline as a control for 4 wk. All mice were then placed on the Paigen diet for 8 wk. The ApoE$^{-/-}$/TRAIL$^{-/-}$ mice that received the recombinant mouse TRAIL demonstrated a significantly elevated RVSP (47.5 ± 6.4 mm Hg) compared with those receiving saline as control (23.0 ± 1.3 mm Hg; Fig. 6 A) and were similar to those observed in ApoE$^{-/-}$ mice fed Paigen diet (Fig. 5 A). Although this was not associated with a significant increase in RVEDP (Fig. 6 B), there was a trend for reduced PA AT (Fig. 6 E) and cardiac index (Fig. 6 F), as well as a significant increase ePVRi (Fig. 6 G). As per Fig. 5, there was no significant effect on left ventricular hemodynamics (Fig. 6, C and D) and no increase in RVH (Fig. 6 H; Table S5).

Published October 15, 2012



There was also a significant increase in pulmonary vascular remodeling comprising SMA-positive cells in the small pulmonary arteries and arterioles of mice receiving recombinant mouse TRAIL (Fig. 6, I and J) compared with the saline-treated mice.

### Treatment of established PAH with an anti-TRAIL antibody increases survival and induces reverse remodeling of disease

Our data thus far provided strong evidence that TRAIL was necessary for the development of PAH in three independent animal models. We next sought to determine whether blocking TRAIL with an anti-TRAIL antibody would have any beneficial effects on slowing disease progression and, ultimately, if it could induce disease regression. We tested this first in the MCT rat model. Rats were injected with MCT and left for 21 d before being randomly assigned into two groups receiving either the anti-TRAIL antibody or IgG control. The antibodies were delivered for 14 d using osmotic mini-pumps. The rats receiving the anti-TRAIL antibody displayed a significant increase in survival compared with IgG control animals (Fig. 7 A). Although there was no significant change in any of the hemodynamic markers of PH or left ventricular hemodynamics (Fig. 7, B–I; Table S2), there was a nonsignificant increase in cardiac index (Fig. 7 G) and a significant reduction in the degree of pulmonary vascular remodeling observed during histological analysis within the anti-TRAIL antibody–treated animals (Fig. 7, J and M). The reduced media/CSA was associated with a significant reduction in vascular proliferation (Fig. 7, K and M), and although there was no significant effect on apoptosis (Fig. 7, L and M), a few apoptotic PASMC were observed (Fig. 7 N). Collectively, these data suggest that there was a partial slowing of disease progression with the anti-TRAIL treatment but no evidence of disease reversal. We next examined whether we could achieve a greater response and induce disease regression using the mouse model. This approach had to two advantages: (1) use of species-specific antibody and (2) implantation of a micro-pump allowing delivery of a twofold higher dose (~0.8 vs. 0.4 ng/g/h) of the anti-TRAIL antibody for twice the duration (4 wk).

After 8 wk of feeding on the Paigen diet, ApoE$^{-/-}$ mice were randomly assigned to two groups and osmotic micropumps were implanted, delivering either anti-TRAIL antibody or IgG for 4 wk. Paigen diet–fed ApoE$^{-/-}$ mice receiving IgG (now 12 wk on diet) displayed a further increase in RVSP compared with the previous study at 8 wk (84.7 ± 25.0 vs. 50.2 ± 3.5 mm Hg). During the study, two mice, one from each group, were sacrificed early (8–10 wk) and failed to make the full 12 wk time course, but their data were included in the full analyses so as not to bias any effects of the treatment. Mice fed Paigen diet for 12 wk and treated with control IgG had severe PAH as demonstrated by dramatically increased RVSP (84.7 ± 25.0 mm Hg, Fig. 8 A), RVEDP (Fig. 8 B), reduced PA AT (Fig. 8 E), and cardiac index (Fig. 8 F) and increased ePVRi (Fig. 8 G). Remarkably, mice that received the anti-TRAIL antibody had a significant reduction in RVSP (29.5 ± 3.1 mm Hg) to near normal levels (Fig. 8 A). Treatment was also associated with a reduction in RVEDP (Fig. 8 B), an increase in both PA AT (Fig. 8 E) and cardiac index (Fig. 8 F), and a significant reduction in ePVRi (Fig. 8 G). As previously described, there was no effect of the Paigen diet on RVH

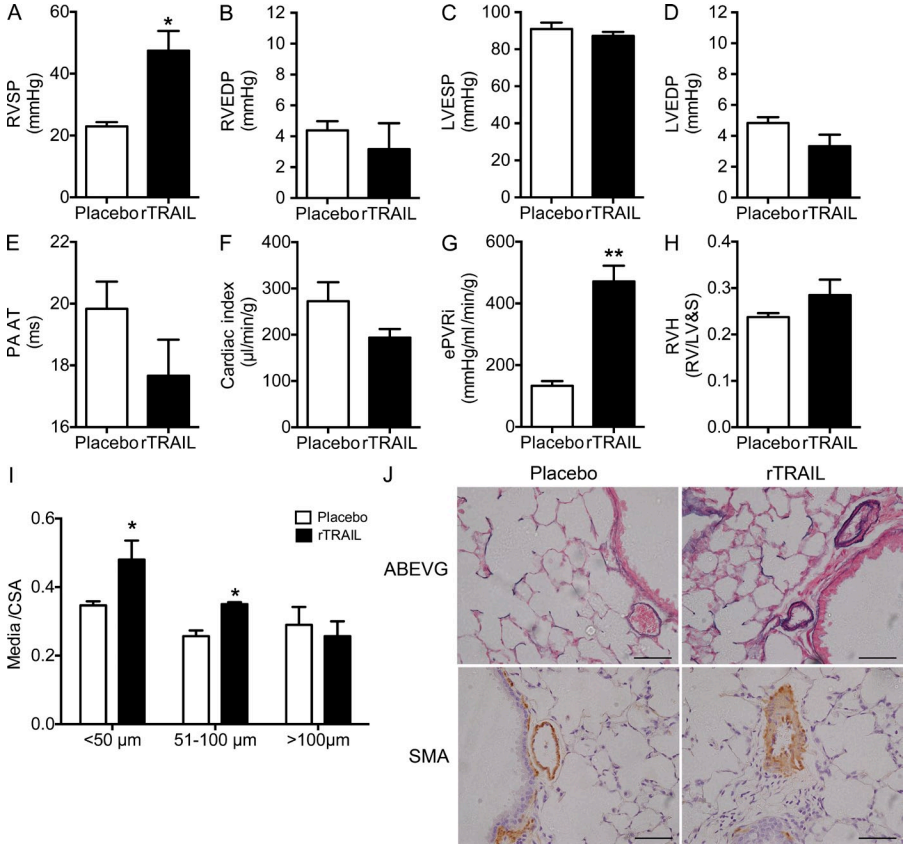


**Figure 6. Addition of recombinant TRAIL to ApoE$^{-/-}$/TRAIL$^{-/-}$ mice reestablished the development of PAH.** (A–D) Bar graphs show RVSP (A), RVEDP (B), LVESP (C), and LVEDP (D), measured in mm Hg. (E–H) PA AT (E), cardiac index (F), ePVRi (G), and RVH (H). (I) The degree of medial wall thickness as a ratio of total vessel size (Media/CSA) in pulmonary arteries <50 µm in diameter. (J) Representative photomicrographs of serial lung sections from ApoE$^{-/-}$/TRAIL$^{-/-}$ mice fed Paigen diet for 8 wk who received either recombinant TRAIL (rTRAIL) or saline (placebo) by osmotic micro-pump for 4 wk. Sections were stained with Alcian Blue Elastic van Gieson (ABEVG) or immunostained for α-SMA. Error bars represent mean ± SEM, $n$ = 4–5 animals per group. *, $P < 0.05$; **, $P < 0.01$ compared with placebo-treated mice. Bars, 50 µm.

Published October 15, 2012



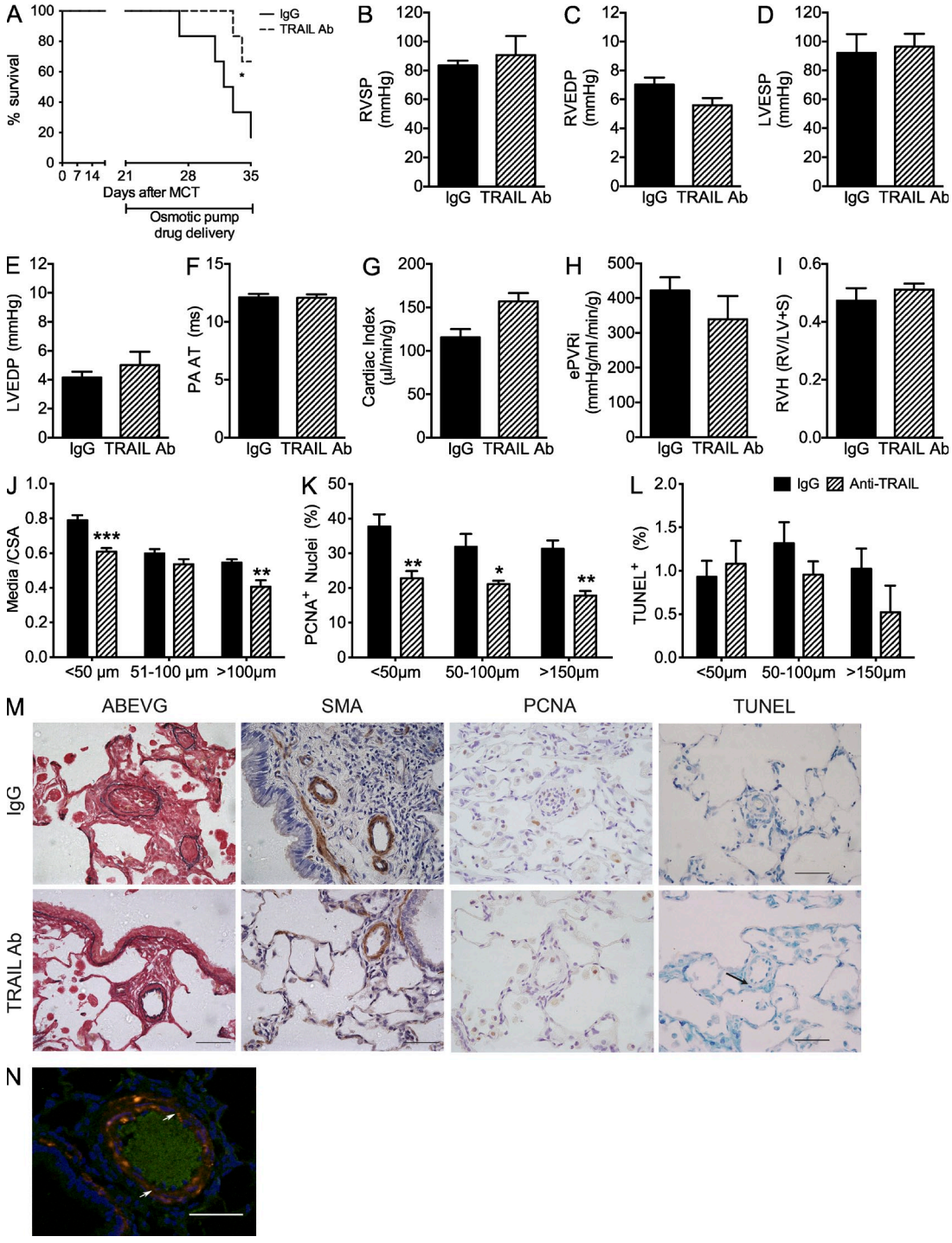


**Figure 7. Anti-TRAIL antibody treatment of established PAH in the MCT rat model prolongs survival and reduces pulmonary vascular remodeling.** (A) Kaplan-Meier plot of survival in IgG and anti-TRAIL–treated rats. (B–E) Bar graphs show RVSP (B), RVEDP (C), LVESP (D), and LVEDP (E), measured in mm Hg. (F–I) PA AT (F), cardiac index (G), ePVRi (H), and RVH (I). (J) The degree of medial wall thickness as a ratio of total vessel size (Media/CSA). (K and L) Quantification of the percentage of proliferating cells (PCNA positive; K), and apoptotic (TUNEL positive; L) separated into pulmonary arteries <50 µm in diameter, vessels from 51 to 100 µm in diameter, and vessels >100 µm in diameter. (M) Representative photomicrographs of serial lung sections from MCT-injected rats treated with either IgG isotype control or an anti-TRAIL antibody. Sections were stained with Alcian Blue Elastic van Gieson (ABEVG) or immunostained for α-SMA, PCNA, or TUNEL. (N) Representative confocal microscopy image showing apoptotic cells (green) and SMC (red) with dual-positive cells (yellow) highlighted by white arrows. Error bars represent mean ± SEM, $n = 6$ animals per group. *, $P < 0.05$; **, $P < 0.01$; ***, $P < 0.001$ compared with IgG-treated MCT-injected rats. Arrows point to TUNEL-positive cells. Bars, 50 µm.

Published October 15, 2012



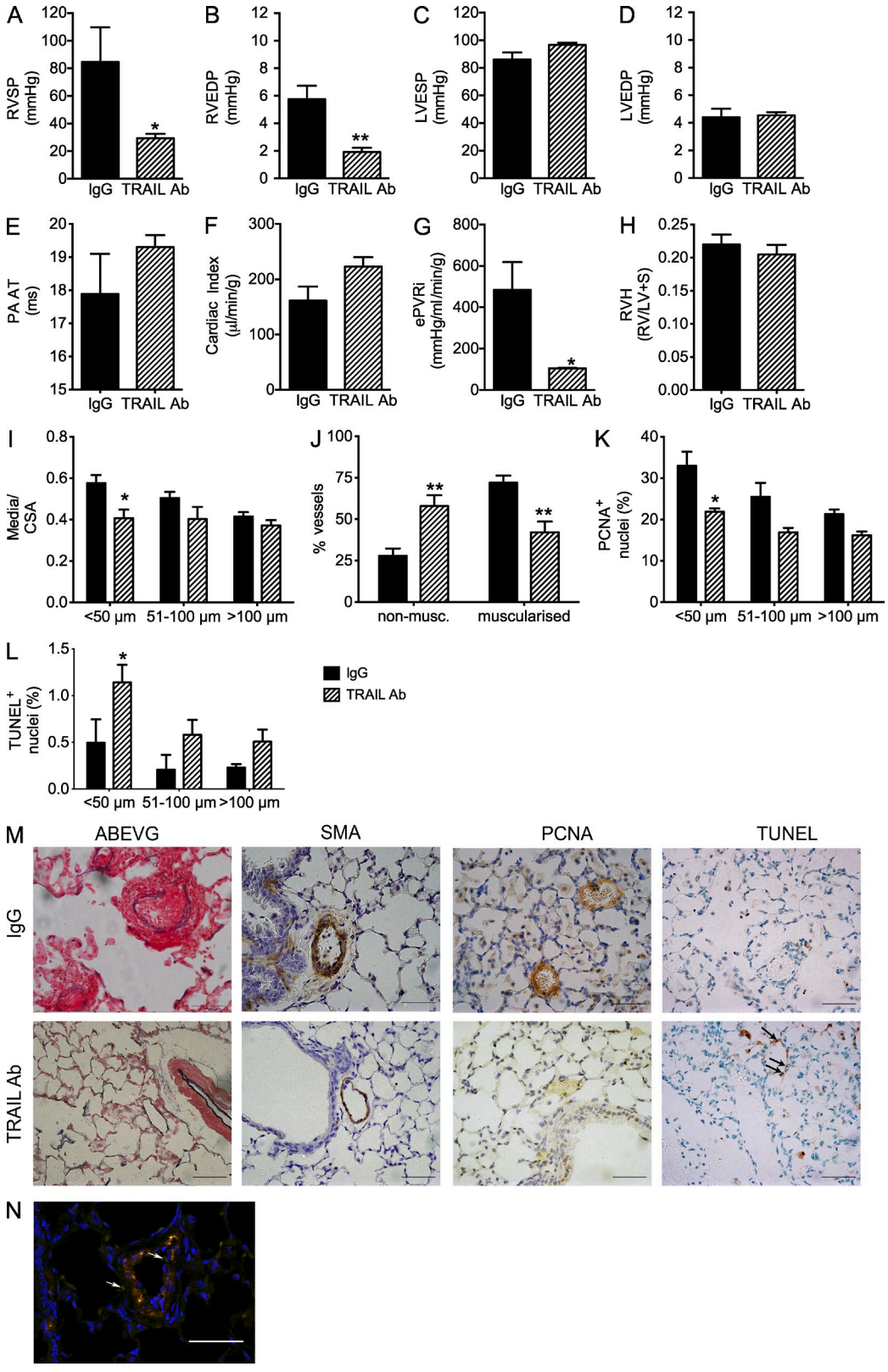


**Figure 8. Anti-TRAIL antibody treatment of established PAH in the Paigen diet–fed ApoE$^{-/-}$ mouse induces disease regression.** (A–D) Bar graphs show RVSP (A), RVEDP (B), LVESP (C), and LVEDP (D), measured in mm Hg. (E–H) PA AT (E), cardiac index (F), ePVRi (G), and RVH (H). (I) The degree of medial wall thickness as a ratio of total vessel size (Media/CSA). (J) Relative percentage of muscularized small pulmonary arteries and arterioles in <50 µm vessels. (K and L) Quantification of the percentage of proliferating cells (PCNA positive; K) and apoptotic (TUNEL positive; L) separated into pulmonary arteries <50 µm in diameter, vessels

Published October 15, 2012



(Fig. 8 H) or left ventricular hemodynamics (Fig. 8, C and D; Table S5). The improvement in hemodynamics was associated with a significant reduction in pulmonary vascular remodeling as assessed by medial/CSA (Fig. 8, I and M) and the percentage of affected vessels (Fig. 8, J and M). Similar to the MCT rat study, there was a significant decrease in the percentage of proliferating cell nuclear antigen (PCNA)–positive cells in the anti-TRAIL–treated animals (Fig. 8, K and M). There was also a significant increase in the number of apoptotic cells within remodeled pulmonary arteries (Fig. 8, L and M), suggesting that the anti-TRAIL treatment both reduced proliferation and induced apoptosis within the remodeled pulmonary arteries. We further identified that the remaining apoptotic cells present within the media of the small pulmonary arteries were SMA positive (Fig. 8 N).

### Tissue expression of TRAIL drives PAH pathogenesis

Because TRAIL is expressed by both circulating inflammatory (e.g., T cells, B cells, neutrophils, and monocytes) and vascular cells, which are both implicated in PAH pathogenesis, we next determined the relative importance of tissue expression of TRAIL compared with circulating BM-derived cells (BMDCs). Before performing these experiments, we confirmed the absence or presence of TRAIL mRNA in ApoE$^{-/-}$ or ApoE$^{-/-}$/TRAIL$^{-/-}$ blood by TaqMan PCR (Fig. 9 A). To perform these studies, we generated four groups of chimeric mice by BM transplantation (BMT). ApoE$^{-/-}$ BM was transplanted (BMT) into sublethally irradiated ApoE$^{-/-}$/TRAIL$^{-/-}$ mice (ApoE$^{-/-}$ into ApoE$^{-/-}$/TRAIL$^{-/-}$) to produce chimeras where TRAIL was only expressed within circulating BMDC, and into ApoE$^{-/-}$ mice as a positive control for the procedure (ApoE$^{-/-}$ into ApoE$^{-/-}$). Conversely, ApoE$^{-/-}$/TRAIL$^{-/-}$ BM was transplanted into sublethally irradiated ApoE$^{-/-}$ mice (ApoE$^{-/-}$/TRAIL$^{-/-}$ into ApoE$^{-/-}$) to generate chimeras where TRAIL was only expressed within the vessel wall, and into ApoE$^{-/-}$/TRAIL$^{-/-}$ (ApoE$^{-/-}$/TRAIL$^{-/-}$ into ApoE$^{-/-}$/TRAIL$^{-/-}$) mice as a negative control. 6 wk after BM reconstitution, mice were randomly placed on either regular chow or Paigen diet. The conversion rate of BMT was 94.9 ± 2.6%. Chow-fed control mice from all BMT groups served as a control for the irradiation and transplant procedure and displayed no PH phenotype. The presence or absence of TRAIL in the recipient lung was confirmed by Western immunoblotting (Fig. 8 B). As previously observed, feeding of the Paigen diet to the ApoE$^{-/-}$ into ApoE$^{-/-}$ and ApoE$^{-/-}$/TRAIL$^{-/-}$ into ApoE$^{-/-}$/TRAIL$^{-/-}$ chimeras recapitulated our findings (Fig. 9, C–M) from the nonirradiated Paigen-fed ApoE$^{-/-}$ and ApoE$^{-/-}$/TRAIL$^{-/-}$ mice (Fig. 5).

The other two groups of chimeric mice with the expression of TRAIL limited to either the tissue or circulating BMDCs displayed disease symptoms after feeding of the Paigen diet and were sacrificed for analysis at 6 wk rather than 8 wk (Fig. 9, C–M). Mice with TRAIL on circulating BMDC, but not in tissue (ApoE$^{-/-}$ into ApoE$^{-/-}$/TRAIL$^{-/-}$), displayed a trend for an increase in RVSP (Fig. 9 C), RVEDP (Fig. 9 D), and PVRi (Fig. 9 H); however, this did not reach statistical significance. Conversely, mice with no TRAIL on circulating BMDC but TRAIL within tissue (ApoE$^{-/-}$/TRAIL$^{-/-}$ into ApoE$^{-/-}$) displayed a significant increase in RVSP (Fig. 9 C), RVEDP (Fig. 9 D), ePVRi (Fig. 9 H), and a significant reduction in cardiac index (Fig. 9 G) that was equivalent to the ApoE$^{-/-}$ into ApoE$^{-/-}$ mice (Table S6). Histological analysis and quantification revealed that the reduced RVSP in the ApoE$^{-/-}$ into ApoE$^{-/-}$/TRAIL$^{-/-}$ chimeras was the result of a reduction in pulmonary artery and arteriole remodeling, both in terms of the number of vessels affected and the degree of muscularization within those affected vessels (Fig. 9, J–M). During these analyses, we observed that some lungs displayed signs of alveolar septa thickening and mild fibrosis, and subsequently applied the modified Ashcroft scoring (Hübner et al., 2008) to all lung sections. Although only mild changes were observed (maximum of 2 from an 8-point scale), interestingly, mice with only TRAIL on circulating cells (ApoE$^{-/-}$ into ApoE$^{-/-}$/TRAIL$^{-/-}$) had no fibrosis and all scored 0 on the modified Ashcroft score (unpublished data).

These data demonstrate that lung tissue expression of TRAIL is the predominate driver of the pulmonary vascular remodeling and the subsequent increase in RVSP that is consistent with the development of PAH in this model, although a role for TRAIL expressed on circulating BMDC cannot be completely dismissed.

## DISCUSSION

In this study, we report for the first time that TRAIL expression is up-regulated in PASMCs isolated from patients with IPAH, and TRAIL is a mitogen and promigratory stimulus for human PASMCs in vitro. Furthermore, we demonstrate through the blockade of TRAIL via either genetic deletion (mice) or with an anti-TRAIL antibody (MCT-treated rat) that TRAIL is required for the development of PAH in three rodent models. Moreover, we have demonstrated the ability of anti-TRAIL antibody treatment to reduce proliferation and increase apoptosis, thereby inducing regression of established pulmonary arterial remodeling and reducing right ventricular pressures.

The number of pharmacological interventions for the treatment of PAH has increased dramatically over the last decade. However, these therapies are restricted principally to targeting three main signaling pathways associated with vasoconstriction, namely endothelin-1, nitric oxide, and prostacyclin (Humbert et al., 2004). Pulmonary vascular vasoconstriction is only one of

from 51 to 100 µm in diameter, and vessels >100 µm in diameter. (M) Representative photomicrographs of serial lung sections from ApoE$^{-/-}$ mice fed on Paigen diet for 12 wk. Sections were stained with Alcian Blue Elastic van Gieson (ABEVG) or immunostained for α-SMA, PCNA, or TUNEL. (N) Representative confocal microscopy image showing apoptotic cells (green) and SMC (red) with dual-positive cells (yellow) highlighted by white arrows. Error bars represent mean ± SEM, $n$ = 4–6 animals per group. *, P < 0.05; **, P < 0.01, compared with IgG-treated Paigen diet-fed mice. Arrows point to TUNEL-positive cells. Bars, 50 µm.

Published October 15, 2012



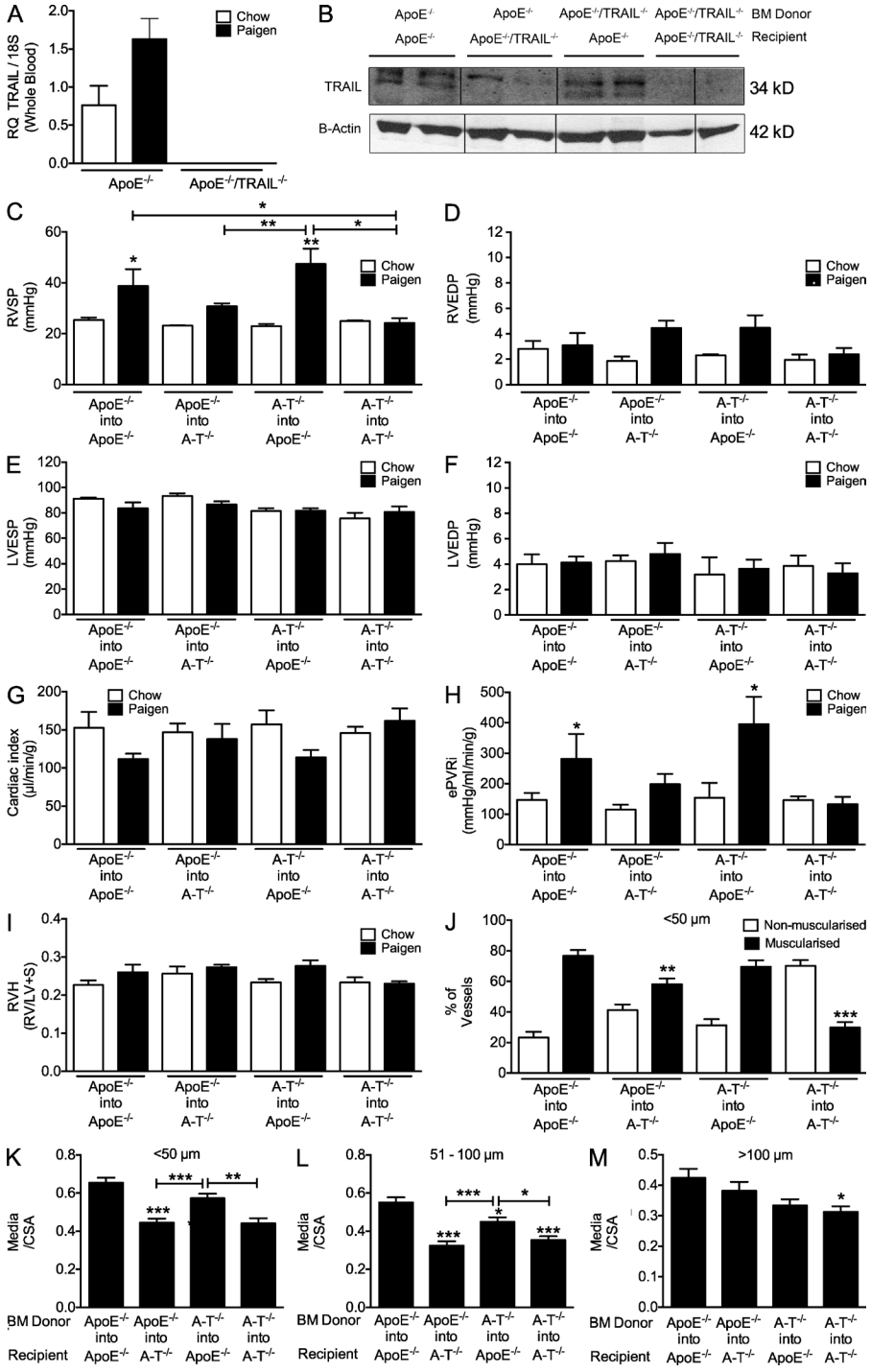


**Figure 9. TRAIL expression within the pulmonary vascular tissue drives PAH in the Paigen diet–fed ApoE$^{-/-}$ mouse.** (A) TaqMan expression of TRAIL in whole blood from ApoE$^{-/-}$ and ApoE$^{-/-}$/TRAIL$^{-/-}$ mice using ΔΔCT with 18S rRNA as the endogenous control gene. Four groups of chimeric mice were generated by BMT. ApoE$^{-/-}$ BM was transplanted into irradiated ApoE$^{-/-}$/TRAIL$^{-/-}$ mice (ApoE$^{-/-}$ into ApoE$^{-/-}$/TRAIL$^{-/-}$) to produce chimeras where TRAIL was only expressed within circulating cells, and into ApoE$^{-/-}$ mice as a positive control for the procedure (ApoE$^{-/-}$ into ApoE$^{-/-}$). Conversely, ApoE$^{-/-}$/TRAIL$^{-/-}$ BM was transplanted into irradiated ApoE$^{-/-}$ mice (ApoE$^{-/-}$/TRAIL$^{-/-}$ into ApoE$^{-/-}$) to generate chimeras where TRAIL was only expressed within the vessel wall, and into ApoE$^{-/-}$/TRAIL$^{-/-}$ (ApoE$^{-/-}$/TRAIL$^{-/-}$ into ApoE$^{-/-}$/TRAIL$^{-/-}$) mice as a negative control. (B) Western immunoblot for TRAIL in whole lung lysates from representative chimeric mice. (C–F) Bar graphs show RVSP (C), RVEDP (D), LVESP (E), and LVEDP (F), measured in mm Hg. (G–I) Cardiac index (G), ePVRi (H), and RVH (I). (J) Relative percentage of muscularized small pulmonary arteries pulmonary arteries <50 µm in diameter, and the degree of medial wall thickness as a ratio of total vessel size (Media/CSA). (K–M) Pulmonary arteries <50 µm in diameter (K), vessels from 51 to 100 µm in diameter (L), and vessels >100 µm in diameter (M). Error bars represent mean ± SEM, $n$ = 3–6 animals per group. *, $P < 0.05$; **, $P < 0.01$; ***, $P < 0.001$, compared chow-fed equivalent mice unless otherwise stated.

the pathophysiological drivers for PAH and, although postulated, there is little proof that any of these drugs have any direct effect on pulmonary vascular proliferation or have the capacity to reverse the proliferative changes in PAH (Schermuly et al., 2005). Although several new targets and drugs have been proposed (Ghofrani et al., 2009), e.g., the inhibition of growth factors such as PDGF that can target the vascular proliferation (Schermuly et al., 2005; Ghofrani et al., 2010), most are generally not specific to the pulmonary circulation. Subsequently, it is clear that despite these new therapeutic approaches there is a need for identification of new specific targets and therapies to reverse this debilitating and fatal disease.

The dogma from early studies in oncology describes TRAIL as a death ligand that can selectively induce apoptosis of transformed tumor cells (Wiley et al., 1995; Pitti et al., 1996). After initial optimism that TRAIL may represent a new therapy for cancer, it is apparent that several cancer cell types have acquired resistance to TRAIL-induced apoptosis in vivo (Wu, 2009). Current strategies now focus on resensitizing tumor cells to the effects of TRAIL with the use of combination therapy.

Since its discovery, several additional roles for TRAIL have been described, particularly in the context of immunoregulatory functions and immune surveillance (Falschlehner et al., 2009; Ikeda et al., 2010). Of particular relevance to our own

Published October 15, 2012



studies has been an emerging body of work supporting an important role for TRAIL in vascular biology, both in the context of interactions between inflammation and vascular cells and via direct effects on VSMC proliferation and migration (Secchiero et al., 2004; Kavurma et al., 2008; Chan et al., 2010). Endothelial cells have also been shown to express TRAIL and its receptors (Pan et al., 1997b; Secchiero et al., 2003), and the role of TRAIL on endothelial cell survival is debated (Gochuico et al., 2000; Malyankar et al., 2000; Li et al., 2003; Secchiero et al., 2003; Zauli and Secchiero, 2006). Interestingly, additional studies have also highlighted a role for TRAIL in the migration of BM stem cells (Secchiero et al., 2008) which have been postulated to contribute to vascular remodeling.

In the context of PAH, there is evidence in the literature that TRAIL expression may be regulated by several pathways associated with PAH, including bone morphogenetic proteins (Nguyen et al., 2007), fibroblast growth factor 2 (FGF2; Chan et al., 2010), and early growth response factor 1 (EGR1; Droin et al., 2003; Fu et al., 2003), all of which are implicated in driving the pathogenesis of PAH (Benisty et al., 2004; Izikki et al., 2009; Morrell et al., 2009; Dickinson et al., 2011; Tu et al., 2011). Interestingly, EGR1 has also been shown to regulate survivin (Wagner et al., 2008) and RAGE (Xu et al., 2010), both of which have been suggested as potential targets for the treatment of PAH (Lawrie et al., 2005; McMurtry et al., 2005; Spiekerkoetter et al., 2009). There is also evidence that peroxisome proliferator-activated receptor γ (PPARγ) activation via agonists rosiglitazone or troglitazone can decrease the expression TRAIL mRNA (Fionda et al., 2007). PPARγ has gained significant recent interest in the context of PAH (Rabinovitch, 2010) and may be particularly pertinent to the mouse model used in this study. Rosiglitazone has been shown to reverse PAH in the ApoE$^{-/-}$ mouse fed a western diet (Hansmann et al., 2007), as well as the hypoxic mouse model (Nisbet et al., 2010). Furthermore, the genetic deletion of PPARγ in either SMCs (Hansmann et al., 2008) or endothelial cells (Guignabert et al., 2009) results in a PAH phenotype in mice by a mechanism involving PDGF and BMP signaling. Conversely, it has been reported that PPARγ can activate membrane TRAIL expression in macrophages (Ho et al., 2011). Similarly, in cancer cells it has been shown that PPARγ agonists can up-regulate the expression of TRAIL receptors and enhance sensitivity to TRAIL-induced apoptosis (Lu et al., 2005; Zou et al., 2007; Bräutigam et al., 2011), suggesting that PPARγ regulation of TRAIL may be tissue and cell specific.

In our current study, data from TRAIL chimeric mice suggest that TRAIL expression by cells in the vessel wall is the main driver in the pathological process. TRAIL is a membrane-anchored protein that can be enzymatically cleaved by cysteine proteases to generate a soluble form of TRAIL (Mariani and Krammer, 1998). Cysteine proteases, including caspases, calpain, and papain, are abundant within the vessel wall (Chapman et al., 1997). Calpain in particular has recently been shown to be important in pulmonary vascular remodeling in animal models of PAH (Ma et al., 2011). Cleavage of TRAIL by cysteine proteinases such as calpain may play an important role in allowing paracrine effects of cleaved soluble TRAIL on multiple cells types. This may also explain why the systemic delivery of recombinant soluble form of TRAIL, without direct presentation by another cell, to Paigen diet–fed ApoE$^{-/-}$/TRAIL$^{-/-}$ mice resulted in the development of a PAH phenotype suggesting that soluble/cleaved levels within the vessel wall are critically important.

Our current study was limited by access to species-specific polyclonal antibodies, so for both intervention studies an anti–mouse TRAIL polyclonal was used. One limitation of the rat studies was that the dose of antibody administered to block the development of PAH in the MCT rat was limited and consequently this may explain the only modest effect on reversal of established disease whether this may have been increased if a higher does of antibody could have been given is not known. To address this concept in the mouse (as reagents were available), we subsequently performed a second reversal study in the mouse with twice the concentration of antibody for twice the duration of treatment. This resulted in normalization of RVSP, significantly reduced pulmonary artery remodeling, and an almost complete reversal in PAH phenotype.

Although there are several limitations of each individual model used, particularly in regard to the mouse, we believe that the combination of three rodent experimental models, each with different disease triggers, add substantial weight to the body of evidence that TRAIL is a key driver in the pulmonary vascular remodeling associated with PAH. We are currently exploring the future therapeutic potential for anti-TRAIL–based therapies.

## MATERIALS AND METHODS

**PASMC RNA from patients with IPAH.** Explanted PASMCs grown in culture from proximal lobar and peripheral arteries (1–2 mm external diameter) from patients with IPAH ($n = 3$) and control ($n = 3$). Smooth muscle phenotype of isolated cells was confirmed by positive immunofluorescence with antibodies to α-SMA, smooth muscle–specific myosin, fibronectin, and vimentin as previously described (Yang et al., 2005). RNA was extracted by TRIzol (Invitrogen). Clinical data on donor is provided in Table S1. All subjects gave informed written consent, and the study was approved by the Local Research Ethics Committee and Papworth Hospital NHS Trust tissue bank, Cambridge, UK.

**TaqMan PCR.** RNA was reverse transcribed using Superscript III (Invitrogen). Gene expression was measured by performing TaqMan PCR using Gene Expression MasterMix and Gene Expression Assays (Applied Biosystems) for TRAIL (Hs00234356_m1), TRAIL-R1 (Hs00269492_m1), TRAIL-R2 (Hs00366278_m1), TRAIL-R3 (Hs00182570_m1), and TRAIL-R4 (Hs04187520_m1). Gene expression was normalized to 18S rRNA (999999011) using the $\Delta\Delta C_T$ comparative quantification method as previously described (Lawrie et al., 2005).

**Cell culture and phenotypic assays.** Human PA-SMCs (Cascade Biologics) were maintained as previously described (Lawrie et al., 2008). Before stimulation, PA-SMCs were synchronized by incubating in DME medium containing PSA Solution (Invitrogen) and 0.2% (vol/vol) fetal bovine serum (Invitrogen) for 48 h. Cell proliferation was assessed using Coulter counting, and migration using a Boyden chamber assay as previously described (Leung et al., 2004). Where stated, cells were stimulated with recombinant human TRAIL or PDGF (both R&D Systems)

**Animals.** Male Sprague Dawley rats were purchased from Charles River. PAH was induced in rats 200–210 g by a single subcutaneous injection of MCT

Published October 15, 2012



(Sigma-Aldrich) at 60 mg/kg. All mice were on a C57BL/6 background. TRAIL$^{-/-}$ mice were originally developed by Amgen/Immunex, obtained as previously described (Watt et al., 2011; Cretney et al., 2002), and obtained by material transfer agreement from Amgen Inc. For the chronic hypoxia model, male TRAIL$^{-/-}$ mice aged 12–13 wk of age (six to eight per group) were placed in hypoxic chambers (10% oxygen) for 2 wk to induce PH. (ApoE$^{-/-}$ (JAX 2052) were obtained from The Jackson Laboratory, and ApoE$^{-/-}$/TRAIL$^{-/-}$ mice were generated in house as previously described (Watt et al., 2011). All mice used were from colonies with greater than six backcrosses. In all experiments, chow-fed, IgG-, or Saline-treated littermate rodents were used as experimental controls. Male mice, 10–12 wk of age (four to seven per group), were fed normal chow (4.3% fat, 0.02% cholesterol, 0.28% sodium) or Paigen diet (18.5% fat, 0.9% cholesterol, 0.5% cholate, and 0.259% sodium) for 8 wk as previously described (Lawrie et al., 2011). Where stated, recombinant mouse TRAIL (rmTRAIL; PeproTech), polyclonal goat anti–mouse TRAIL (anti-TRAIL), or control goat IgG isotype antibodies (R&D Systems) were delivered to rodents through subcutaneously implanted osmotic pumps (Durect Corp.). Interventions were delivered via an Alzet 1004 micro pump (100 µl reservoir, 0.1 µl/h for 4 wk) in mice and via an Alzet 2002 mini-pump (200 µl reservoir, 0.5 µl/h for 2 wk) in rats. Antibodies were delivered at 84 ng/h (~0.4 ng/g/h) in rats and 20 ng/h (0.8 ng/g/h) in mice; rmTRAIL was administered at 10 ng/h (0.4 ng/g/h). For the rat survival studies animals, right heart failure (RHF) served as the survival end point. RHF was defined by loss of body weight (either >5%/24 h or >10%/48 h), lethargy, and respiratory distress as previously described (Merklinger et al., 2005; de Man et al., 2012). All animal experiments were approved by the University of Sheffield Project Review Committee and conformed to UK Home Office ethical guidelines.

**BMT.** BMT was performed as previously described (Chamberlain et al., 2006). In brief, male mice, 6–8 wk old, received a sublethal dose of whole-body irradiation (1,100 rads, split into two doses, 4 h apart). Irradiated recipients then received three to four million cells, isolated from 4–6-wk-old mice in Hanks' balanced salt solution, by tail-vein injection. After 6 wks of recovery on regular chow, mice were randomly assigned to chow or Paigen diets for a further 8 wk as described in the Animals section.

**Echocardiography.** Echocardiography was performed using the Vevo 770 system (Visual Sonics) using either the RMV707B (mice) or RMV710B (rat) scan head. Rodents were placed on a heated platform and covered to minimize heat loss. Rectal temperature, heart rate and respiratory rate were recorded continuously throughout the study. Anesthesia was induced and maintained using Isoflurane through oxygen maintaining heart rates at ~450–500 (mice) and 325–350 (rats) beats per minute (bpm), whenever possible. The rodents were depilated and preheated ultrasound gel was applied (Aquasonics 100 Gel; Parker Laboratories Inc.), and echocardiography was performed and analyzed as previously described (Lawrie et al., 2011) with PA AT reported as data supportive of our cardiac catheter data throughout the manuscript.

**Cardiac catheterization.** After echocardiography, left and right ventricular catheterization was performed using a closed chest method via the right internal carotid artery and right external jugular vein under isoflurane-induced anesthesia, as previously described (Lawrie et al., 2011). Data were collected using an ultra-miniature pressure-volume PVR-1045 1F catheter (mouse LV), PVR-1030 (Mouse RV), and SPR-838 2F catheter (rat LV) SPR-847 1.4F catheter (rat RV; Millar Instruments Inc.) coupled to a Millar MPVS 300 and a PowerLab 8/30 data acquisition system (AD Instruments) and recorded using Chart v7 software (AD Instruments). Pressure volume analysis was performed using PVAN (v2.3; Millar Instruments Inc). We subsequently calculated an ePVRi by estimating mean PAP (EmPAP) from the RVSP by adapting the equation from Chemla et al. (2004) and substituting the systolic PA pressure for RVSP to give [EmPAP = (0.61 × RVSP) + 2 mm Hg]. EmPAP was then substitute for mPAP in the PVRi equation described by McMurtry et al. (2005; mPAP–left ventricular end-diastolic pressure [LVEDP]/cardiac index).

**RVH.** RVH was measured by calculating the ratio of the right ventricular free wall over left ventricle plus septum.

**Immunohistochemistry.** Immediately after harvest, the left lung was perfusion fixed via the trachea with 10% (vol/vol) formal buffered saline by inflation to 20 cm of $H_2O$. The lungs were then processed into paraffin blocks for sectioning. Paraffin-embedded sections (5 µm) of lung were histologically stained for Alcian Blue Elastin van Gieson (ABEVG), immunohistochemically stained for α-SMA (M0851; Dako) to visualize SMCs and von Willebrand Factor (vWF; A0082; Dako) to visualize endothelial cells, and TRAIL (ab2435; Abcam) was also used to localize protein expression to pulmonary vascular lesions. To assess proliferation, slides were stained with a mouse anti–human PCNA antibody (M0879; Dako). A secondary biotinylated anti–mouse antibody (1:200) was added before an Avidin Biotin enzyme Complex (Vectastain kit; Vector Laboratories). All protocols used 3,3 diaminobenzidine as the substrate for color in the peroxidase reaction and counterstained with hematoxylin.

Apoptotic nuclei were detected with a TdT-mediated dUTP nick-end labeling (TUNEL) assay using a colorimetric DNA fragmentation detection kit (fragEL; QIA33; EMD Millipore; Merck) according to the manufacturer's instruction and counterstained with methyl green. To further define apoptotic cells, we used the Fluorescein in situ Cell Death Detection kit (Roche) with Alexa Fluor 555 secondary antibody to detect α-SMA (M0851). Images were captured on an inverted confocal and multiphoton microscope (LSM 510 NLO; Carl Zeiss). For both the Fluorescein and Alexa Fluor 555, we used an HFT488/543/633 dichroic mirror with an NFT545 beam splitter and a 488 nm Argon laser for Fluorescein with a 500–530 band pass filter, a 543 HeNe for Alexa Fluor 555 with a 565–615 nm band pass filter, a Coherent Chameleon laser tuned to 740 nm for multiphoton excitation, a KP650 dichroic mirror, a BG39 IR filter, and a spectral detector set to collect 394–480 nm light for the detection of DAPI. The specimens were scanned using each laser/fluorescence channel sequentially to reduce the risk of fluorescence artifacts.

**Quantification of pulmonary vascular remodeling.** Pulmonary vascular remodeling was quantified by assessing the degree of muscularization and the percentage of affected pulmonary arteries and arterioles in three groups based on vessel size: small pulmonary arterioles with a diameter <50 µm, medium pulmonary arteries with a range in diameter from 51 to 100 µm, and large pulmonary arteries with a diameter >100 µm, and standard immunohistochemical techniques were applied as previously described (Lawrie et al., 2011). In all cases, both IgG and no primary antibody negative controls were used.

**Western immunoblotting.** 20 µg of each sample was loaded on a 4–12% Bis-Tris NuPage gel and run under reducing conditions in MES running buffer (Invitrogen) before transfer to a nitrocellulose membrane (Invitrogen). Transfer was confirmed with Ponceau S (Sigma-Aldrich) staining and the membrane was then blocked for 1 h in 5% nonfat milk at room temperature. The blots were incubated with either phospho-p44/42 MAPK (Erk1/2; Thr202/Tyr204) rabbit monoclonal antibody (Cell Signaling Technology), p44/42 MAPK (Erk1/2) mouse monoclonal antibody (Cell Signaling Technology), or anti–b-Actin mouse monoclonal antibody (Abcam) for 1 h at room temperature, or anti-TRAIL rabbit polyclonal antibody (Abcam) overnight at 4°C. For detection of p44/42, horseradish peroxidase (HRP)–conjugated anti–mouse and anti–rabbit antibodies (1:5000; GE Healthcare) were incubated for 1 h at room temperature before performing an enhanced chemiluminescence (ECL; GE Healthcare) reaction and exposure to autoradiographic film (GE Healthcare). For detection of TRAIL and b-Actin, fluorescently labeled anti–rabbit (IR Dye 800CW; LI-COR Biosciences) and anti–mouse (IRDye 680RD) were incubated for 1 h at room temperature before reading at 700/800 nm on an Odyssey SA imaging system (LI-COR Biosciences).

**Statistical analyses.** Statistical analysis was performed using either a Mann-Whitney test when comparing two groups, or a Kruskal-Wallis followed by the Dunns post-hoc test with a 95% confidence level. $P < 0.05$ was deemed statistically significant (Prism 4.0c for Macintosh; GraphPad Software).

**Online supplemental material.** Additional information on patient phenotype is available in the online supplement. Online supplemental material is available at http://www.jem.org/cgi/content/full/jem.20112716/DC1.

We would like to acknowledge technical assistance from Mrs. Tatiana Vinogradova. TRAIL−/− mice were obtained under MTA # 200908042 from Amgen Inc., Thousand Oaks, CA, USA.

Funding for this study was provided by Medical Research Council Career Development Award (G0800318, A. Lawrie); British Heart Foundation Clinical Research Training Fellowship (FS/08/061/25740, A.G. Hameed); National Institute for Health Research Sheffield Cardiovascular Biomedical Research Unit (N.D. Arnold, J.A. Pickworth, and D.C. Crossman); and Cambridge National Institutes for Health Research Biomedical Research Centre. Wellcome Trust Vacation Scholarships were awarded to S. Dawson and A. Reva.

None of the authors have any competing financial interests in relation to this work.

**Submitted: 20 December 2011**
**Accepted: 24 September 2012**

## REFERENCES

Ashkenazi, A., and V.M. Dixit. 1998. Death receptors: signaling and modulation. *Science*. 281:1305–1308. http://dx.doi.org/10.1126/science.281.5381.1305

Benisty, J.I., V.V. McLaughlin, M.J. Landzberg, J.D. Rich, J.W. Newburger, S. Rich, and J. Folkman. 2004. Elevated basic fibroblast growth factor levels in patients with pulmonary arterial hypertension. *Chest*. 126:1255–1261. http://dx.doi.org/10.1378/chest.126.4.1255

Bräutigam, K., J. Biernath-Wüpping, D.O. Bauerschlag, C.S. von Kaisenberg, W. Jonat, N. Maass, N. Arnold, and I. Meinhold-Heerlein. 2011. Combined treatment with TRAIL and PPARγ ligands overcomes chemoresistance of ovarian cancer cell lines. *J. Cancer Res. Clin. Oncol.* 137:875–886. http://dx.doi.org/10.1007/s00432-010-0952-2

Chamberlain, J., D. Evans, A. King, R. Dewberry, S. Dower, D. Crossman, and S. Francis. 2006. Interleukin-1beta and signaling of interleukin-1 in vascular wall and circulating cells modulates the extent of neointima formation in mice. *Am. J. Pathol.* 168:1396–1403. http://dx.doi.org/10.2353/ajpath.2006.051054

Chan, J., L. Prado-Lourenco, L.M. Khachigian, M.R. Bennett, B.A. Di Bartolo, and M.M. Kavurma. 2010. TRAIL promotes VSMC proliferation and neointima formation in a FGF-2-, Sp1 phosphorylation-, and NFkappaB-dependent manner. *Circ. Res.* 106:1061–1071. http://dx.doi.org/10.1161/CIRCRESAHA.109.206029

Chapman, H.A., R.J. Riese, and G.P. Shi. 1997. Emerging roles for cysteine proteases in human biology. *Annu. Rev. Physiol.* 59:63–88. http://dx.doi.org/10.1146/annurev.physiol.59.1.63

Chemla, D., V. Castelain, M. Humbert, J.-L. Hébert, G. Simonneau, Y. Lecarpentier, and P. Hervé. 2004. New formula for predicting mean pulmonary artery pressure using systolic pulmonary artery pressure. *Chest*. 126:1313–1317. http://dx.doi.org/10.1378/chest.126.4.1313

Chin, K.M., N.H.S. Kim, and L.J. Rubin. 2005. The right ventricle in pulmonary hypertension. *Coron. Artery Dis.* 16:13–18. http://dx.doi.org/10.1097/00019501-200502000-00003

Cretney, E., K. Takeda, H. Yagita, M. Glaccum, J.J. Peschon, and M.J. Smyth. 2002. Increased susceptibility to tumor initiation and metastasis in TNF-related apoptosis-inducing ligand-deficient mice. *J. Immunol.* 168:1356–1361.

de Man, F.S., M.L. Handoko, J.J.M. van Ballegoij, I. Schalij, S.J.P. Bogaards, P.E. Postmus, J. van der Velden, N. Westerhof, W.J. Paulus, and A. Vonk-Noordegraaf. 2012. Bisoprolol delays progression towards right heart failure in experimental pulmonary hypertension. *Circ. Heart Fail.* 5:97–105. http://dx.doi.org/10.1161/CIRCHEARTFAILURE.111.964494

De Toni, E.N., S.E. Thieme, A. Herbst, A. Behrens, P. Stieber, A. Jung, H. Blum, B. Göke, and F.T. Kolligs. 2008. OPG is regulated by beta-catenin and mediates resistance to TRAIL-induced apoptosis in colon cancer. *Clin. Cancer Res.* 14:4713–4718. http://dx.doi.org/10.1158/1078-0432.CCR-07-5019

Degli-Esposti, M.A., W.C. Dougall, P.J. Smolak, J.Y. Waugh, C.A. Smith, and R.G. Goodwin. 1997a. The novel receptor TRAIL-R4 induces NF-kappaB and protects against TRAIL-mediated apoptosis, yet retains an incomplete death domain. *Immunity*. 7:813–820. http://dx.doi.org/10.1016/S1074-7613(00)80399-4

Degli-Esposti, M.A., P.J. Smolak, H. Walczak, J. Waugh, C.P. Huang, R.F. DuBose, R.G. Goodwin, and C.A. Smith. 1997b. Cloning and characterization of TRAIL-R3, a novel member of the emerging TRAIL receptor family. *J. Exp. Med.* 186:1165–1170. http://dx.doi.org/10.1084/jem.186.7.1165

Dickinson, M.G., B. Bartelds, G. Molema, M.A. Borgdorff, B. Boersma, J. Takens, M. Weij, P. Wichers, H. Sietsma, and R.M.F. Berger. 2011. Egr-1 expression during neointimal development in flow-associated pulmonary hypertension. *Am. J. Pathol.* 179:2199–2209. http://dx.doi.org/10.1016/j.ajpath.2011.07.030

Droin, N.M., M.J. Pinkoski, E. Dejardin, and D.R. Green. 2003. Egr family members regulate nonlymphoid expression of Fas ligand, TRAIL, and tumor necrosis factor during immune responses. *Mol. Cell. Biol.* 23:7638–7647. http://dx.doi.org/10.1128/MCB.23.21.7638-7647.2003

Emery, J.G., P. McDonnell, M.B. Burke, K.C. Deen, S. Lyn, C. Silverman, E. Dul, E.R. Appelbaum, C. Eichman, R. DiPrinzio, et al. 1998. Osteoprotegerin is a receptor for the cytotoxic ligand TRAIL. *J. Biol. Chem.* 273:14363–14367. http://dx.doi.org/10.1074/jbc.273.23.14363

Falschlehner, C., U. Schaefer, and H. Walczak. 2009. Following TRAIL's path in the immune system. *Immunology*. 127:145–154. http://dx.doi.org/10.1111/j.1365-2567.2009.03058.x

Fionda, C., F. Nappi, M. Piccoli, L. Frati, A. Santoni, and M. Cippitelli. 2007. Inhibition of trail gene expression by cyclopentenonic prostaglandin 15-deoxy-delta12,14-prostaglandin J2 in T lymphocytes. *Mol. Pharmacol.* 72:1246–1257. http://dx.doi.org/10.1124/mol.107.038042

Fu, M., X. Zhu, J. Zhang, J. Liang, Y. Lin, L. Zhao, M.U. Ehrengruber, and Y.E. Chen. 2003. Egr-1 target genes in human endothelial cells identified by microarray analysis. *Gene*. 315:33–41. http://dx.doi.org/10.1016/S0378-1119(03)00730-3

Ghofrani, H.A., R.J. Barst, R.L. Benza, H.C. Champion, K.A. Fagan, F. Grimminger, M. Humbert, G. Simonneau, D.J. Stewart, C. Ventura, and L.J. Rubin. 2009. Future perspectives for the treatment of pulmonary arterial hypertension. *J. Am. Coll. Cardiol.* 54:S108–S117. http://dx.doi.org/10.1016/j.jacc.2009.04.014

Ghofrani, H.A., N.W. Morrell, M.M. Hoeper, H. Olschewski, A.J. Peacock, R.J. Barst, S. Shapiro, H. Golpon, M. Toshner, F. Grimminger, and S. Pascoe. 2010. Imatinib in pulmonary arterial hypertension patients with inadequate response to established therapy. *Am. J. Respir. Crit. Care Med.* 182:1171–1177. http://dx.doi.org/10.1164/rccm.201001-0123OC

Gochuico, B.R., J. Zhang, B.Y. Ma, A. Marshak-Rothstein, and A. Fine. 2000. TRAIL expression in vascular smooth muscle. *Am. J. Physiol. Lung Cell. Mol. Physiol.* 278:L1045–L1050.

Guignabert, C., C.M. Alvira, T.-P. Alastalo, H. Sawada, G. Hansmann, M. Zhao, L. Wang, N. El-Bizri, and M. Rabinovitch. 2009. Tie2-mediated loss of peroxisome proliferator-activated receptor-gamma in mice causes PDGF receptor-beta-dependent pulmonary arterial muscularization. *Am. J. Physiol. Lung Cell. Mol. Physiol.* 297:L1082–L1090. http://dx.doi.org/10.1152/ajplung.00199.2009

Hagen, M., K. Fagan, W. Steudel, M. Carr, K. Lane, D.M. Rodman, and J. West. 2007. Interaction of interleukin-6 and the BMP pathway in pulmonary smooth muscle. *Am. J. Physiol. Lung Cell. Mol. Physiol.* 292:L1473–L1479. http://dx.doi.org/10.1152/ajplung.00197.2006

Hansmann, G., R.A. Wagner, S. Schellong, V.A. Perez, T. Urashima, L. Wang, A.Y. Sheikh, R.S. Suen, D.J. Stewart, and M. Rabinovitch. 2007. Pulmonary arterial hypertension is linked to insulin resistance and reversed by peroxisome proliferator-activated receptor-gamma activation. *Circulation*. 115:1275–1284.

Hansmann, G., V.A. de Jesus Perez, T.-P. Alastalo, C.M. Alvira, C. Guignabert, J.M. Bekker, S. Schellong, T. Urashima, L. Wang, N.W. Morrell, and M. Rabinovitch. 2008. An antiproliferative BMP-2/PPARgamma/apoE axis in human and murine SMCs and its role in pulmonary hypertension. *J. Clin. Invest.* 118:1846–1857. http://dx.doi.org/10.1172/JCI32503

Hemnes, A.R., and H.C. Champion. 2008. Right heart function and haemodynamics in pulmonary hypertension. *Int. J. Clin. Pract. Suppl.* 62:11–19. http://dx.doi.org/10.1111/j.1742-1241.2008.01812.x

Ho, T.C., S.L. Chen, S.C. Shih, S.J. Chang, S.L. Yang, J.W. Hsieh, H.C. Cheng, L.J. Chen, and Y.P. Tsao. 2011. Pigment epithelium-derived factor (PEDF) promotes tumor cell death by inducing macrophage membrane tumor necrosis factor-related apoptosis-inducing ligand (TRAIL). *J. Biol. Chem.* 286:35943–35954. http://dx.doi.org/10.1074/jbc.M111.266064

Holen, I., and C.M. Shipman. 2006. Role of osteoprotegerin (OPG) in cancer. *Clin. Sci.* 110:279–291. http://dx.doi.org/10.1042/CS20050175

Hopkins-Donaldson, S., A. Ziegler, S. Kurtz, C. Bigosch, D. Kandioler, C. Ludwig, U. Zangemeister-Wittke, and R. Stahel. 2003. Silencing of death receptor and caspase-8 expression in small cell lung carcinoma cell lines and tumors by DNA methylation. *Cell Death Differ.* 10:356–364. http://dx.doi.org/10.1038/sj.cdd.4401157

Hübner, R.-H., W. Gitter, N.E. El Mokhtari, M. Mathiak, M. Both, H. Bolte, S. Freitag-Wolf, and B. Bewig. 2008. Standardized quantification of pulmonary fibrosis in histological samples. *Biotechniques.* 44:507–511: 514–517. http://dx.doi.org/10.2144/000112729

Humbert, M. 2008. Update in pulmonary arterial hypertension 2007. *Am. J. Respir. Crit. Care Med.* 177:574–579. http://dx.doi.org/10.1164/rccm.200801-029UP

Humbert, M., and V.V. McLaughlin. 2009. The 4th World Symposium on Pulmonary Hypertension. Introduction. *J. Am. Coll. Cardiol.* 54:S1–S2. http://dx.doi.org/10.1016/j.jacc.2009.04.013

Humbert, M., G. Monti, F. Brenot, O. Sitbon, A. Portier, L. Grangeot-Keros, P. Duroux, P. Galanaud, G. Simonneau, and D. Emilie. 1995. Increased interleukin-1 and interleukin-6 serum concentrations in severe primary pulmonary hypertension. *Am. J. Respir. Crit. Care Med.* 151:1628–1631.

Humbert, M., O. Sitbon, and G. Simonneau. 2004. Treatment of pulmonary arterial hypertension. *N. Engl. J. Med.* 351:1425–1436. http://dx.doi.org/10.1056/NEJMra040291

Ikeda, T., S. Hirata, S. Fukushima, Y. Matsunaga, T. Ito, M. Uchino, Y. Nishimura, and S. Senju. 2010. Dual effects of TRAIL in suppression of autoimmunity: the inhibition of Th1 cells and the promotion of regulatory T cells. *J. Immunol.* 185:5259–5267. http://dx.doi.org/10.4049/jimmunol.0902797

International PPH Consortium, Lane, K.B., R.D. Machado, M.W. Pauciulo, J.R. Thomson, J.A. Phillips III, J.E. Loyd, W.C. Nichols, and R.C. Trembath. 2000. Heterozygous germline mutations in BMPR2, encoding a TGF-beta receptor, cause familial primary pulmonary hypertension. *Nat. Genet.* 26:81–84. http://dx.doi.org/10.1038/79226

Izikki, M., C. Guignabert, E. Fadel, M. Humbert, L. Tu, P. Zadigue, P. Dartevelle, G. Simonneau, S. Adnot, B. Maitre, et al. 2009. Endothelial-derived FGF2 contributes to the progression of pulmonary hypertension in humans and rodents. *J. Clin. Invest.* 119:512–523. http://dx.doi.org/10.1172/JCI35070

Kavurma, M.M., M. Schoppet, Y.V. Bobryshev, L.M. Khachigian, and M.R. Bennett. 2008. TRAIL stimulates proliferation of vascular smooth muscle cells via activation of NF-kappaB and induction of insulin-like growth factor-1 receptor. *J. Biol. Chem.* 283:7754–7762. http://dx.doi.org/10.1074/jbc.M706927200

Lawrie, A., E. Spiekerkoetter, E.C. Martinez, N. Ambartsumian, W.J. Sheward, M.R. MacLean, A.J. Harmar, A.-M. Schmidt, E. Lukanidin, and M. Rabinovitch. 2005. Interdependent serotonin transporter and receptor pathways regulate S100A4/Mts1, a gene associated with pulmonary vascular disease. *Circ. Res.* 97:227–235. http://dx.doi.org/10.1161/01.RES.0000176025.57706.1e

Lawrie, A., E. Waterman, M. Southwood, D. Evans, J. Suntharalingam, S. Francis, D.C. Crossman, P. Croucher, N.W. Morrell, and C. Newman. 2008. Evidence of a role for osteoprotegerin in the pathogenesis of pulmonary arterial hypertension. *Am. J. Pathol.* 172:256–264. http://dx.doi.org/10.2353/ajpath.2008.070395

Lawrie, A., A.G. Hameed, J. Chamberlain, N. Arnold, A. Kennerley, K. Hopkinson, J. Pickworth, D.G. Kiely, D.C. Crossman, and S.E. Francis. 2011. Paigen diet-fed apolipoprotein E knockout mice develop severe pulmonary hypertension in an interleukin-1-dependent manner. *Am. J. Pathol.* 179:1693–1705. http://dx.doi.org/10.1016/j.ajpath.2011.06.037

LeBlanc, H.N., and A. Ashkenazi. 2003. Apo2L/TRAIL and its death and decoy receptors. *Cell Death Differ.* 10:66–75. http://dx.doi.org/10.1038/sj.cdd.4401187

Lee, S.L., W.W. Wang, G.A. Finlay, and B.L. Fanburg. 1999. Serotonin stimulates mitogen-activated protein kinase activity through the formation of superoxide anion. *Am. J. Physiol.* 277:L282–L291.

Leung, W.C.Y., A. Lawrie, S. Demaries, H. Massaeli, A. Burry, S. Yablonsky, J.M. Sarjeant, E. Fera, E. Rassart, J.G. Pickering, and M. Rabinovitch. 2004. Apolipoprotein D and platelet-derived growth factor-BB synergism mediates vascular smooth muscle cell migration. *Circ. Res.* 95:179–186. http://dx.doi.org/10.1161/01.RES.0000135482.74178.14

Li, J.H., N.C. Kirkiles-Smith, J.M. McNiff, and J.S. Pober. 2003. TRAIL induces apoptosis and inflammatory gene expression in human endothelial cells. *J. Immunol.* 171:1526–1533.

Long, L., M.R. MacLean, T.K. Jeffery, I. Morecroft, X. Yang, N. Rudarakanchana, M. Southwood, V. James, R.C. Trembath, and N.W. Morrell. 2006. Serotonin increases susceptibility to pulmonary hypertension in BMPR2-deficient mice. *Circ. Res.* 98:818–827. http://dx.doi.org/10.1161/01.RES.0000215809.47923.fd

Lu, M., T. Kwan, C. Yu, F. Chen, B. Freedman, J.M. Schafer, E.-J. Lee, J.L. Jameson, V.C. Jordan, and V.L. Cryns. 2005. Peroxisome proliferator-activated receptor gamma agonists promote TRAIL-induced apoptosis by reducing survivin levels via cyclin D3 repression and cell cycle arrest. *J. Biol. Chem.* 280:6742–6751. http://dx.doi.org/10.1074/jbc.M411519200

Ma, W., W. Han, P.A. Greer, R.M. Tuder, H.A. Toque, K.K.W. Wang, R.W. Caldwell, and Y. Su. 2011. Calpain mediates pulmonary vascular remodeling in rodent models of pulmonary hypertension, and its inhibition attenuates pathologic features of disease. *J. Clin. Invest.* 121:4548–4566. http://dx.doi.org/10.1172/JCI57734

MacFarlane, M., M. Ahmad, S.M. Srinivasula, T. Fernandes-Alnemri, G.M. Cohen, and E.S. Alnemri. 1997. Identification and molecular cloning of two novel receptors for the cytotoxic ligand TRAIL. *J. Biol. Chem.* 272:25417–25420. http://dx.doi.org/10.1074/jbc.272.41.25417

Malyankar, U.M., M. Scatena, K.L. Suchland, T.J. Yun, E.A. Clark, and C.M. Giachelli. 2000. Osteoprotegerin is an alpha vbeta 3-induced, NF-kappa B-dependent survival factor for endothelial cells. *J. Biol. Chem.* 275:20959–20962. http://dx.doi.org/10.1074/jbc.C000290200

Mariani, S.M., and P.H. Krammer. 1998. Differential regulation of TRAIL and CD95 ligand in transformed cells of the T and B lymphocyte lineage. *Eur. J. Immunol.* 28:973–982. http://dx.doi.org/10.1002/(SICI)1521-4141(199803)28:03<973::AID-IMMU973>3.0.CO;2-T

Marsters, S.A., J.P. Sheridan, R.M. Pitti, A. Huang, M. Skubatch, D. Baldwin, J. Yuan, A. Gurney, A.D. Goddard, P. Godowski, and A. Ashkenazi. 1997. A novel receptor for Apo2L/TRAIL contains a truncated death domain. *Curr. Biol.* 7:1003–1006. http://dx.doi.org/10.1016/S0960-9822(06)00422-2

McGrath, E.E., H.M. Marriott, A. Lawrie, S.E. Francis, I. Sabroe, S.A. Renshaw, D.H. Dockrell, and M.K.B. Whyte. 2011. TNF-related apoptosis-inducing ligand (TRAIL) regulates inflammatory neutrophil apoptosis and enhances resolution of inflammation. *J. Leukoc. Biol.* 90:855–865. http://dx.doi.org/10.1189/jlb.0211062

McMurtry, M.S., S.L. Archer, D.C. Altieri, S. Bonnet, A. Haromy, G. Harry, S. Bonnet, L. Puttagunta, and E.D. Michelakis. 2005. Gene therapy targeting survivin selectively induces pulmonary vascular apoptosis and reverses pulmonary arterial hypertension. *J. Clin. Invest.* 115:1479–1491. http://dx.doi.org/10.1172/JCI23203

Merklinger, S.L., P.L. Jones, E.C. Martinez, and M. Rabinovitch. 2005. Epidermal growth factor receptor blockade mediates smooth muscle cell apoptosis and improves survival in rats with pulmonary hypertension. *Circulation.* 112:423–431. http://dx.doi.org/10.1161/CIRCULATIONAHA.105.540542

Miyashita, T., A. Kawakami, T. Nakashima, S. Yamasaki, M. Tamai, F. Tanaka, M. Kamachi, H. Ida, K. Migita, T. Origuchi, et al. 2004. Osteoprotegerin (OPG) acts as an endogenous decoy receptor in tumour necrosis factor-related apoptosis-inducing ligand (TRAIL)-mediated apoptosis of fibroblast-like synovial cells. *Clin. Exp. Immunol.* 137:430–436. http://dx.doi.org/10.1111/j.1365-2249.2004.02534.x

Morrell, N.W., S. Adnot, S.L. Archer, J. Dupuis, P.L. Jones, M.R. MacLean, I.F. McMurtry, K.R. Stenmark, P.A. Thistlethwaite, N. Weissmann, et al. 2009. Cellular and molecular basis of pulmonary arterial hypertension. *J. Am. Coll. Cardiol.* 54:S20–S31. http://dx.doi.org/10.1016/j.jacc.2009.04.018

Nguyen, K.Q., P. Olesen, T. Ledet, and L.M. Rasmussen. 2007. Bone morphogenetic proteins regulate osteoprotegerin and its ligands in

human vascular smooth muscle cells. *Endocrine*. 32:52–58. http://dx.doi.org/10.1007/s12020-007-9007-0

Nisbet, R.E., J.M. Bland, D.J. Kleinhenz, P.O. Mitchell, E.R. Walp, R.L. Sutliff, and C.M. Hart. 2010. Rosiglitazone attenuates chronic hypoxia-induced pulmonary hypertension in a mouse model. *Am. J. Respir. Cell Mol. Biol.* 42:482–490. http://dx.doi.org/10.1165/rcmb.2008-0132OC

Pai, S.I., G.S. Wu, N. Ozören, L. Wu, J. Jen, D. Sidransky, and W.S. El-Deiry. 1998. Rare loss-of-function mutation of a death receptor gene in head and neck cancer. *Cancer Res.* 58:3513–3518.

Pan, G., J. Ni, Y.F. Wei, G. Yu, R. Gentz, and V.M. Dixit. 1997a. An antagonist decoy receptor and a death domain-containing receptor for TRAIL. *Science*.277:815–818.http://dx.doi.org/10.1126/science.277.5327.815

Pan, G., K. O'Rourke, A.M. Chinnaiyan, R. Gentz, R. Ebner, J. Ni, and V.M. Dixit. 1997b. The receptor for the cytotoxic ligand TRAIL. *Science*. 276:111–113. http://dx.doi.org/10.1126/science.276.5309.111

Pan, G., J. Ni, G. Yu, Y.F. Wei, and V.M. Dixit. 1998. TRUNDD, a new member of the TRAIL receptor family that antagonizes TRAIL signalling. *FEBS Lett.* 424:41–45. http://dx.doi.org/10.1016/S0014-5793(98)00135-5

Perros, F., D. Montani, P. Dorfmüller, I. Durand-Gasselin, C. Tcherakian, J. Le Pavec, M. Mazmanian, E. Fadel, S. Mussot, O. Mercier, et al. 2008. Platelet-derived growth factor expression and function in idiopathic pulmonary arterial hypertension. *Am. J. Respir. Crit. Care Med.* 178:81–88. http://dx.doi.org/10.1164/rccm.200707-1037OC

Pitti, R.M., S.A. Marsters, S. Ruppert, C.J. Donahue, A. Moore, and A. Ashkenazi. 1996. Induction of apoptosis by Apo-2 ligand, a new member of the tumor necrosis factor cytokine family. *J. Biol. Chem.* 271:12687–12690. http://dx.doi.org/10.1074/jbc.271.22.12687

Rabinovitch, M. 2010. PPARgamma and the pathobiology of pulmonary arterial hypertension. *Adv. Exp. Med. Biol.* 661:447–458. http://dx.doi.org/10.1007/978-1-60761-500-2_29

Schermuly, R.T., E. Dony, H.A. Ghofrani, S. Pullamsetti, R. Savai, M. Roth, A. Sydykov, Y.J. Lai, N. Weissmann, W. Seeger, and F. Grimminger. 2005. Reversal of experimental pulmonary hypertension by PDGF inhibition. *J. Clin. Invest.* 115:2811–2821. http://dx.doi.org/10.1172/JCI24838

Screaton, G.R., J. Mongkolsapaya, X.N. Xu, A.E. Cowper, A.J. McMichael, and J.I. Bell. 1997. TRICK2, a new alternatively spliced receptor that transduces the cytotoxic signal from TRAIL. *Curr. Biol.* 7:693–696. http://dx.doi.org/10.1016/S0960-9822(06)00297-1

Secchiero, P., A. Gonelli, E. Carnevale, D. Milani, A. Pandolfi, D. Zella, and G. Zauli. 2003. TRAIL promotes the survival and proliferation of primary human vascular endothelial cells by activating the Akt and ERK pathways. *Circulation*. 107:2250–2256. http://dx.doi.org/10.1161/01.CIR.0000062702.60708.C4

Secchiero, P., C. Zerbinati, E. Rimondi, F. Corallini, D. Milani, V. Grill, G. Forti, S. Capitani, and G. Zauli. 2004. TRAIL promotes the survival, migration and proliferation of vascular smooth muscle cells. *Cell. Mol. Life Sci.* 61:1965–1974. http://dx.doi.org/10.1007/s00018-004-4197-6

Secchiero, P., E. Melloni, F. Corallini, A.P. Beltrami, F. Alviano, D. Milani, F. D'Aurizio, M.G. di Iasio, D. Cesselli, G.P. Bagnara, and G. Zauli. 2008. Tumor necrosis factor-related apoptosis-inducing ligand promotes migration of human bone marrow multipotent stromal cells. *Stem Cells*. 26:2955–2963. http://dx.doi.org/10.1634/stemcells.2008-0512

Simoncini, S., M.-S. Njock, S. Robert, L. Camoin-Jau, J. Sampol, J.-R. Harlé, C. Nguyen, F. Dignat-George, and F. Anfosso. 2009. TRAIL/Apo2L mediates the release of procoagulant endothelial microparticles induced by thrombin in vitro: a potential mechanism linking inflammation and coagulation. *Circ. Res.* 104:943–951. http://dx.doi.org/10.1161/CIRCRESAHA.108.183285

Song, S., K. Choi, S.-W. Ryu, S.W. Kang, and C. Choi. 2011. TRAIL promotes caspase-dependent pro-inflammatory responses via PKCδ activation by vascular smooth muscle cells. *Cell Death Dis.* 2:e223. http://dx.doi.org/10.1038/cddis.2011.103

Spiekerkoetter, E., C. Guignabert, V. de Jesus Perez, T.-P. Alastalo, J.M. Powers, L. Wang, A. Lawrie, N. Ambartsumian, A.-M. Schmidt, M. Berryman, et al. 2009. S100A4 and bone morphogenetic protein-2 codependently induce vascular smooth muscle cell migration via phospho-extracellular signal-regulated kinase and chloride intracellular channel 4. *Circ. Res.* 105:639–647: 13: 647. http://dx.doi.org/10.1161/CIRCRESAHA.109.205120

Steiner, M.K., O.L. Syrkina, N. Kolliputi, E.J. Mark, C.A. Hales, and A.B. Waxman. 2009. Interleukin-6 overexpression induces pulmonary hypertension. *Circ. Res.* 104:236–244: 28p: 244. http://dx.doi.org/10.1161/CIRCRESAHA.108.182014

Tang, W., W. Wang, Y. Zhang, S. Liu, Y. Liu, and D. Zheng. 2009. TRAIL receptor mediates inflammatory cytokine release in an NF-kappaB-dependent manner. *Cell Res.* 19:758–767. http://dx.doi.org/10.1038/cr.2009.57

Tu, L., L. Dewachter, B. Gore, E. Fadel, P. Dartevelle, G. Simonneau, M. Humbert, S. Eddahibi, and C. Guignabert. 2011. Autocrine fibroblast growth factor-2 signaling contributes to altered endothelial phenotype in pulmonary hypertension. *Am. J. Respir. Cell Mol. Biol.* 45:311–322. http://dx.doi.org/10.1165/rcmb.2010-0317OC

Wagner, M., K. Schmelz, B. Dörken, and I. Tamm. 2008. Transcriptional regulation of human survivin by early growth response (Egr)-1 transcription factor. *Int. J. Cancer.* 122:1278–1287. http://dx.doi.org/10.1002/ijc.23183

Walczak, H., M.A. Degli-Esposti, R.S. Johnson, P.J. Smolak, J.Y. Waugh, N. Boiani, M.S. Timour, M.J. Gerhart, K.A. Schooley, C.A. Smith, et al. 1997. TRAIL-R2: a novel apoptosis-mediating receptor for TRAIL. *EMBO J.* 16:5386–5397. http://dx.doi.org/10.1093/emboj/16.17.5386

Wang, P., Y. Lu, C. Li, N. Li, P. Yu, and D. Ma. 2011. Novel transcript variants of TRAIL show different activities in activation of NF-κB and apoptosis. *Life Sci.* 89:839–846. http://dx.doi.org/10.1016/j.lfs.2011.09.003

Watt, V., J. Chamberlain, T. Steiner, S. Francis, and D. Crossman. 2011. TRAIL attenuates the development of atherosclerosis in apolipoprotein E deficient mice. *Atherosclerosis*. 215:348–354. http://dx.doi.org/10.1016/j.atherosclerosis.2011.01.010

Wiley, S.R., K. Schooley, P.J. Smolak, W.S. Din, C.P. Huang, J.K. Nicholl, G.R. Sutherland, T.D. Smith, C. Rauch, C.A. Smith, et al. 1995. Identification and characterization of a new member of the TNF family that induces apoptosis. *Immunity*. 3:673–682. http://dx.doi.org/10.1016/1074-7613(95)90057-8

Wu, G.S. 2009. TRAIL as a target in anti-cancer therapy. *Cancer Lett.* 285:1–5. http://dx.doi.org/10.1016/j.canlet.2009.02.029

Wu, G.S., T.F. Burns, Y. Zhan, E.S. Alnemri, and W.S. El-Deiry. 1999. Molecular cloning and functional analysis of the mouse homologue of the KILLER/DR5 tumor necrosis factor-related apoptosis-inducing ligand (TRAIL) death receptor. *Cancer Res.* 59:2770–2775.

Xu, Y., F. Toure, W. Qu, L. Lin, F. Song, X. Shen, R. Rosario, J. Garcia, A.-M. Schmidt, and S.-F. Yan. 2010. Advanced glycation end product (AGE)-receptor for AGE (RAGE) signaling and up-regulation of Egr-1 in hypoxic macrophages. *J. Biol. Chem.* 285:23233–23240. http://dx.doi.org/10.1074/jbc.M110.117457

Yang, X., L. Long, M. Southwood, N. Rudarakanchana, P.D. Upton, T.K. Jeffery, C. Atkinson, H. Chen, R.C. Trembath, and N.W. Morrell. 2005. Dysfunctional Smad signaling contributes to abnormal smooth muscle cell proliferation in familial pulmonary arterial hypertension. *Circ. Res.* 96:1053–1063. http://dx.doi.org/10.1161/01.RES.0000166926.54293.68

Zauli, G., and P. Secchiero. 2006. The role of the TRAIL/TRAIL receptors system in hematopoiesis and endothelial cell biology. *Cytokine Growth Factor Rev.* 17:245–257. http://dx.doi.org/10.1016/j.cytogfr.2006.04.002

Zou, W., X. Liu, P. Yue, F.R. Khuri, and S.-Y. Sun. 2007. PPARgamma ligands enhance TRAIL-induced apoptosis through DR5 upregulation and c-FLIP downregulation in human lung cancer cells. *Cancer Biol. Ther.* 6:99–106. http://dx.doi.org/10.4161/cbt.6.1.3555